





Effect of glass powder on the rheological and mechanical properties of slag-based mechanochemical activation geopolymer grout

Mukhtar Hamid Abed, Israa Sabbar Abbas & Hanifi Canakci

To cite this article: Mukhtar Hamid Abed, Israa Sabbar Abbas & Hanifi Canakci (2022): Effect of glass powder on the rheological and mechanical properties of slag-based mechanochemical activation geopolymer grout, European Journal of Environmental and Civil Engineering, DOI: [10.1080/19648189.2022.2145374](https://doi.org/10.1080/19648189.2022.2145374)

To link to this article: <https://doi.org/10.1080/19648189.2022.2145374>

 View supplementary material [↗](#)

 Published online: 08 Dec 2022.

 Submit your article to this journal [↗](#)




 Article views: 37

 View related articles [↗](#)

 View Crossmark data [↗](#)



Effect of glass powder on the rheological and mechanical properties of slag-based mechanochemical activation geopolymer grout

Mukhtar Hamid Abed^{a,b} , Israa Sabbar Abbas^{a,c}  and Hanifi Canakci^d 

^aDepartment of Civil Engineering, Gaziantep University, Gaziantep, Turkey; ^bProjects Department, Al Ramadi Municipality, Anbar, Iraq; ^cDepartment of Civil Engineering, Al-Qalam University College, Kirkuk, Iraq; ^dDepartment of Civil Engineering, Hasan Kalyoncu University, Gaziantep, Turkey

ABSTRACT

This article discusses the effects of glass powder (GP) replacements and sodium hydroxide (NaOH) molarity on the rheological, fresh, mechanical and microstructure characteristics of slag-based mechanochemical geopolymer (MG) grout. A conventionally activated geopolymer grout and an ordinary Portland cement (OPC) grout were also investigated for comparison. Four glass powder replacement ratios were used (0%, 10%, 20% and 30% by the total precursor weight) to prepare slag-based mechanochemical geopolymer at three NaOH concentrations (1.25, 2.5 and 3.75 molars). The experimental results showed that the rheological behaviour of MG grouts was considerably reduced, whereas the setting time and the bleeding capacity value increased when slag was substituted with 0%–30% GP. However, after 28 days, the unconfined compressive strength (UCS) improved by 2%–13% when 10%–20% GP was used as a slag replacement, then dropped by 4% when 30% GP was substituted. The results confirmed that both geopolymer grouts irrespective of the activation method had shorter setting time and more stable bleeding capacity than OPC grout. The results also revealed that the UCS of geopolymer grout is enhanced by 18% when the source materials are activated by the mechanochemical method compared to the conventional activation of geopolymer grout. The microstructure results revealed that the activation method had a considerable effect on the microstructure of geopolymer grout because the ball milling process increased the surface area and reduced the particle size of slag compared to conventionally activated geopolymer grout.

ARTICLE HISTORY

Received 18 May 2022
Accepted 29 October 2022


KEYWORDS

Glass powder; mechanochemical activation; rheological; bleeding capacity; setting time; microstructure

1. Introduction

Nowadays, geopolymer materials have shown sufficient potential to be utilised as an OPC alternative (Juenger et al., 2011). The geopolymerisation process between an aluminosilicate source (precursor) and an alkali activator forms a geopolymer, resulting in an amorphous microstructure (Nedunuri & Muhammad, 2020). Geopolymer materials are eco-friendly, chemically resistant, durable, have excellent mechanical properties, resist alkali-aggregate reactions and show viscoplastic behaviour similar to traditional OPC (Humur & Çevik, 2022; Bilondi et al., 2018; Favier et al., 2014; Pacheco-Torgal et al., 2011; Palacios et al., 2008; Humur & Çevik, 2022). Despite the geopolymer binder's extraordinary environmental potential, its utilisation has so

CONTACT Mukhtar Hamid Abed  eng.mukhtar92@gmail.com  Department of Civil Engineering, Gaziantep University, Gaziantep, Turkey; Israa Sabbar Abbas  israasabbar52@gmail.com  Department of Civil Engineering, Gaziantep University, Gaziantep, Turkey.

 Supplemental data for this article can be accessed online at <https://doi.org/10.1080/19648189.2022.2145374>

far been limited to small-scale applications due to heat curing and hazardous alkaline activators. Geopolymers should be used widely in the construction industry to maximise their environmental friendliness. Conventional geopolymers are produced using a two-part process that includes alkaline solutions and solid alumina-silica precursors. These hazardous activators are frequently utilised to dissolve the alumina-silica raw ingredients and control the geopolymer's mechanical characteristics (Lee & Van Deventer, 2002; Lee & Van Deventer, 2003). Some deficiencies are associated with the two-part mix formulations utilised to synthesise 'conventional' geopolymer (Duxson & Provis, 2008). The handling of the alkali solution is risky and prone to on-site hazardous accidents. Furthermore, the geopolymer's rheology may be complex and difficult to control due to the formation of a sticky slurry and thick material, particularly in geopolymer systems, including sodium as an alkali source (Provis, 2009). To facilitate the commercialisation of geopolymeric materials on a wide scale, it is critical to replace this conventional activation approach because it is not a user-friendly process. Sodium hydroxide dissolution in water is an exothermic reaction that results in the formation of a hazardous alkaline solution. Therefore, an alternative activation method should be developed to overcome these limitations by using geopolymer materials in a solid form similar to OPC. Solid form geopolymers are an innovative approach to alleviating the challenges associated with conventional geopolymeric systems and eliminating the need to handle highly alkaline solutions activating geopolymers.

Mechanochemical activation is a method for manufacturing geopolymers via an innovative solid-state chemistry mechanism that involves co-grinding small particles of solid matter to create molecular, reactive, dense and amorphous aggregated composite particles (Gupta et al., 2017). It requires solid binders, such as aluminosilicate source and alkaline activators, which are combined in a ball mill and, as such, require only water to commence the geopolymerisation process (Hosseini et al., 2021). The intense grinding or milling process can introduce defects and electrostatic charges onto the surface of the particles, increasing the surface energy and causing crystalline to amorphous phase changes (Intini et al., 2009; Baláz et al., 2013) and activated particle agglomeration (Souri et al., 2015). Besides, mechanical activation can increase reactivity and improve the geopolymerisation rate (Temuujin et al., 2009; Kumar & Kumar, 2011). The mechanochemical approach is used in this research to ease the utilisation of geopolymer materials and to serve as an alternative activation technique for addressing the drawbacks of traditional geopolymer activation. Limited investigations have been addressed the performance of geopolymer activated by mechanochemical activation method so far. Kushwah et al., (2021) developed a solid form geopolymeric binder by ball-milling aluminosilicate precursors with dry activators. The geopolymeric precursors were made by initiating a reaction between an alkaline solution and alumina-silicates sources. The results indicated that the effect of ball-milling duration was significant from 2 h to 6 h, and the strength was considerably enhanced; however, the strength was negatively reduced when the grinding duration was higher than 6 h (8, 10 and 12 h). Mukhtar et al. (2022a) investigated the rheological and mechanical differences between the mechanochemical activation approach and its conventional counterpart. The experimental results revealed that the mechanochemical activation technique lowered the rheological properties (i.e. initial apparent viscosity reduced by 38%) of geopolymer grout compared to the conventional activation process, whereas the mechanical properties were significantly enhanced. Hosseini et al., (2021) indicated that mechanochemical activation enhanced the dispersion of bottom ash-fly ash particles, altered the Na_2SiO_3 and aluminosilicate reaction kinetics, intensified the interconnectivity of geopolymer structure, and decreased pore size; thus, the compressive strength significantly increased between 60% and 80%. Gupta et al., (2017) reported that the mechanochemical reactions between fly ash and sodium hydroxide in the dry state considerably improved the mechanical performance of geopolymer systems.

To the best of the author's knowledge, the previously published studies only focussed on fly ash and slag-based-mechanochemical geopolymer; however, the other waste materials such as glass powder, rice husk ash and metakaolin, remain unexplored. Therefore, this study focuses on the effect of glass powder replacement on the performance of slag-based mechanochemical geopolymers. Waste glass has attracted increased interest as a source of SiO_2 -bearing municipal solid waste in the preparation of geopolymers. The traditional alumina-silicate byproducts such as slag and fly ash are no longer considered as waste but commercial products in the cement manufacturing industry (Xiao et al., 2020). Therefore, the majority of waste glass is still disposed of in landfills nowadays is a promising raw material in the alkaline activation process (Xiao et al., 2020; Zhang et al., 2020). Additionally, waste glass has been found to contain more than 70% amorphous silica and has a relatively stable chemical composition, which is essential because soda-lime glass constitutes the majority of industrially manufactured glass (Xiao et al., 2020; Xiao

et al., 2020; Si et al., 2020). Several recent research has highlighted the effectiveness of GP as a pozzolanic material for aluminosilicates in alkaline-activated materials, owing to its affinity for high dissolution in alkali environments (Khan et al., 2021; Liu et al., 2019). Samarakoon et al., (2020) showed that the workability and strength of the alkaline-activated binders gradually increased with an increasing amount of substitution of fly ash by glass powder, and a significant improvement in setting time and flow was seen with the addition of glass powder. Morphological and elemental analysis revealed an improvement of the microstructure of alkali-activated binders due to the increased formation of calcium-dominant hydration products and hence reduced porosity with the substitution of glass powder. Li et al., (2020) investigated the rheology response of one-part alkaline activated slag/glass powder pastes and discovered that when more slag was substituted for glass powder, the plastic viscosity, yield stress and strength performance of the one-part alkali activated paste reduced while the flow and setting time values increased. Si et al., (2020) reported that replacing 10% and 20% GP increased the elastic modulus of the resulting gel. Additionally, specimens with 5% GP demonstrated the highest compressive strength of all samples examined. Also, their study revealed that the appropriate glass powder replacement could affect the geopolymerisation process and the gels generated in the metakaolin-based geopolymer, thus increasing the mixture's mechanical characteristics.

This study examines the effects of glass powder replacement and molar concentration of NaOH on the performance of mechanochemical geopolymer grout. A conventionally activated geopolymer-based grout and an ordinary Portland cement (OPC) grout were also investigated for comparison. Rheological properties (flow curve response, yield stress and plastic viscosity), fresh characteristics (setting time and bleeding capacity), mechanical characteristics (unconfined compressive strength, ultrasonic pulse velocity) and microstructure analysis (scanning electronic microscopy) were tested for all the studied types of grouts.

2. Experimental work

2.1. Materials

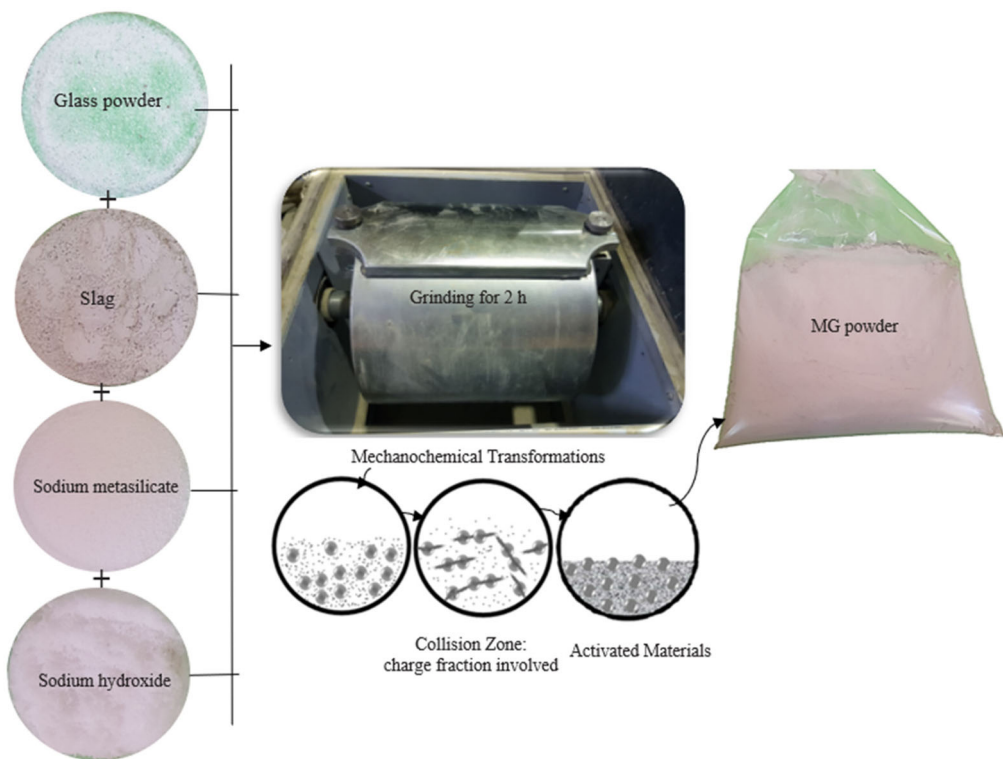
Slag and glass powder (GP) were used in this research to produce a mechanochemical geopolymer. The slag is obtained from the iron and steel industry (Iskenderun Iron and Steel Plant in Hatay province, Turkey), and the GP is obtained from green soda-lime bottles collected primarily from shops in Gaziantep, Turkey. The waste green soda-lime bottles were first washed with tap water to remove labels from the exterior of the glass and then cleaned inside to remove impurities. The waste green soda-lime bottles were naturally dried in the laboratory for 24 hours and grounded to powder using a Los Angeles abrasion machine. Finally, the glass powder passed the No. 35 sieve with a particle size less than 0.5 mm and was adapted for the mechanochemical activation process. Also, CEM I-42.5R Portland cement in accordance with ASTM C150 was used to produce Portland cement grout for comparison purposes. The combination of NaOH and sodium silicate as alkaline activators was chosen in this research. Sodium hydroxide pellets with a purity of 98% were locally obtained. The ratio of sodium metasilicate powder (Na_2SiO_3 -Penta) to sodium hydroxide is 0.5. Table 1 summarises the physicochemical characteristics of the OPC, precursor components (slag and GP) and Na_2SiO_3 .

2.2 Samples preparation

In this study, the mechanochemical activation (co-grinding NaOH, sodium metasilicate, slag and glass powder for 2 hours) was carried out in an 80 kg ball mill equipped with 12 balls with a diameter of 45 mm and a mass of 400 g. During the co-grinding process, the particles of source materials are trapped between the balls and chamber walls and subjected to continuous impact and milling; the collision between the tiny rigid balls in a container generates localised high pressure (Figure 1). This causes a decrease in particle size, an increase in specific surface area, a reduction in crystallinity, a change in the mineralogy and an increase in the amorphous phase (Mukhtar et al., 2022a). After that, the obtained geopolymeric precursors are mixed with faucet water to create MG grout. It is worth noting that the grinding period for the geopolymeric precursors was set at 2 h based on previous studies (Kushwah et al., 2021; Mukhtar et al., 2022a; Matalkah et al., 2017; Masi et al., 2021). In this study, specimen's names (MG-GP0, MG-GP10, MG-GP20 and MG-GP 30) are denoted with specific codes. The labels MG and GP represent mechanochemical geopolymer grout and glass powder, respectively, and the numbers '0', '10', '20' and

Table 1. Physical and chemical characteristics of OPC, slag, GP and Na₂SiO₃.

Constituent (%)	OPC	Slag	GP	(Na ₂ SiO ₃ -Penta) Powder
a) Chemical composition				
CaO	62.58	34.19	8.21	
Al ₂ O ₃	5.31	10.6	1.0	
SiO ₂	20.25	40.42	78	28
Fe ₂ O ₃	4.04	1.28	0.52	
MgO	2.82	7.63	0.14	
SO ₃	2.73	0.68	0.6	
K ₂ O	0.92	0.0128	0.09	
Na ₂ O	0.22		12	29
Modulus ratio				1
H ₂ O				43
b) Physical properties				
Specific gravity	3.15	2.9	2.54	
Specific surface (m ² /kg)	326	565	382	

**Figure 1.** The mechanochemical activation process.

'30' indicate the percentage of glass powder content in the slag mechanochemical geopolymer grout by weight. For comparison, slag-based conventional geopolymer grout (CG) (to examine the effect of the activation method) and ordinary Portland cement grout were prepared. Furthermore, various concentration of NaOH was chosen (1.25 M, 2.5 M and 3.75 M) to examine the effect of the NaOH concentration on the rheological performance and mechanical behaviour of MG grout. In the case of conventional slag-based geopolymer grout preparations, NaOH beads were calculated and weighed at a molarity of 3.75 and dissolved in faucet water. During the mixing time, an exothermic reaction occurred, and the NaOH solution became extremely hot. Because of this, the liquid was kept at room temperature prior to use until chemical equilibrium was achieved, and then the Na₂SiO₃ was added after the sodium hydroxide liquid cooled.

The alkaline activator solution was generally prepared at least 24 h prior to the mixing of geopolymer components. After that, the alkali solution was mixed with slag to synthesis conventional geopolymer

grout (CG). Also, OPC was mixed with water (the same water amount that used to prepare MG grout at 3.75 M) in order to produce OPC grout for comparison purposes. The mix proportions of all studied mixes are summarised in Table 2.

2.3 Testing methods

All grout mixtures were prepared in the laboratory at a temperature of $23 \pm 3^\circ\text{C}$. Rheological experiments were conducted in accordance with (Fluids, 2003) utilising a rational viscometer (proRheo R .180). The grout mixtures were unable to produce flow responses at shear rates less than 500 s^{-1} during the viscometer trials. Thus, shear rates ranging from 500 s^{-1} to 1000 s^{-1} (Figure 2) were used to investigate the flow responses of shear stress and apparent viscosity of grout (Güllü & Agha, 2021; Güllü et al., 2019; Güllü et al., 2021). All shear rates were maintained for a duration of 15 s in order to achieve an equilibrium condition in a total of 120 s for each mixture.

The flow curves of shear stress and apparent viscosity vs shear rate were determined for both portions (descending and ascending). Nevertheless, the ascending portion of data was considered in this research since their trend lines correspond to an undisturbed condition (Şahmaran, 2008; Yahia & Khayat, 2001; Park et al., 2005; Widjaja & Lee, 2013). In this research, a modified Bingham model was used to determine the yield stress and plastic viscosity based on previous investigations (Şahmaran, 2008; Yahia & Khayat, 2001; Yahia et al., 2016), as described in Equation (1):

$$\tau = \tau_0 + \mu_p \dot{\gamma} + C \dot{\gamma}^2 \quad (1)$$

where τ is the shear stress (Pa), μ_p is the plastic viscosity (Pa.s), τ_0 is the yield stress (Pa) and C is a constant. In the modified Bingham model, the ratio of the second-order term to the linear term could be used to characterise a nonlinear response, indicating shear thickening, shear thinning, and the Bingham model for $C > 0$, $C < 0$ and $C = 0$, respectively (Güllü, 2016; Feys et al., 2013; Rifaai et al., 2019).

Regarding fresh properties, the setting time was measured by conducting Vicat needle tests in accordance with ASTM C191-19 (American Society for Testing & Materials, 1987) recommendations. According to ASTM C940-16 (ASTM:C940-10a, 2010), bleeding capacity tests were conducted to show the grout stability. The fresh grouts were placed in a graduated cylinder (1000 mL) for 120 min. Then, the volume of bleed water was measured every 30 min interval until observation time was reached.

In order to obtain mechanical characteristics, the fresh grout was cast into cylindrical moulds with a height of 10 cm and diameter of 5 cm to examine the unconfined compressive strength for geopolymer grouts in accordance with standards (ASTM:D2938-95, 1995). The grout specimens were kept at room temperature for 7 days and 28 days. Before conducting the UCS tests, the specimens were utilised to determine the wave velocity using ultrasonic pulse velocity (UPV) (ASTM, 2009). The UCS tests of the specimens were uniaxially loaded under displacement control at the rate of 1 mm/min. The peak axial stress measured at failure was accounted for the UCS value. The magnitude of UPV measurements can

Table 2. Mix proportions of grout.

Molarity	Mix ID	Weight: %						Weight: (g)					
		Slag %	GP %	NaOH %	OPC %	Na ₂ SiO ₃ %	Grinding duration: h	Slag (g)	GP (g)	NaOH (g)	Na ₂ SiO ₃ (g)	OPC (g)	Water (g)
1.25	MG-GP0	85	0	10	-	5	2	850	0	100	50	-	1250
	MG-GP10	75	10	10	-	5	2	750	100	100	50	-	1250
	MG-GP20	65	20	10	-	5	2	650	200	100	50	-	1250
	MG-GP30	55	30	10	-	5	2	550	300	100	50	-	1250
2.5	MG-GP0	85	0	10	-	5	2	850	0	100	50	-	1000
	MG-GP10	75	10	10	-	5	2	750	100	100	50	-	1000
	MG-GP20	65	20	10	-	5	2	650	200	100	50	-	1000
	MG-GP30	55	30	10	-	5	2	550	300	100	50	-	1000
3.75	MG-GP0	85	0	10	-	5	2	850	0	100	50	-	750
	MG-GP10	75	10	10	-	5	2	750	100	100	50	-	750
	MG-GP20	65	20	10	-	5	2	650	200	100	50	-	750
	MG-GP30	55	30	10	-	5	2	550	300	100	50	-	750
-	CG	85	0	10	-	5	-	850	0	100	50	-	750
-	OPC	-	-	-	100	-	-	-	-	-	-	1000	750

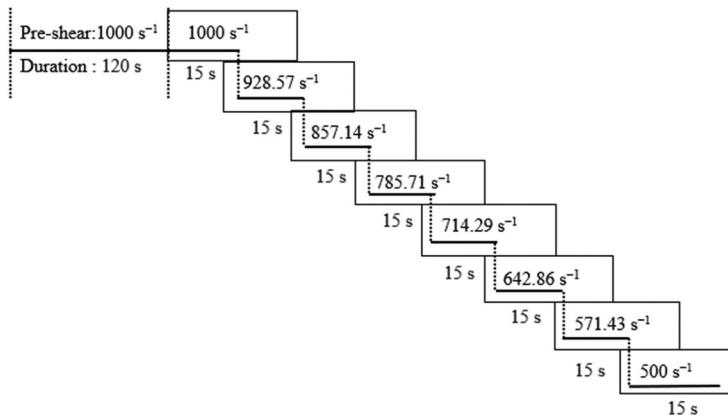


Figure 2. The shear rate protocol was applied to draw the flow curves of grout.

Table 3. UPV classification (Anon, 1979).

UPV (m/s)	Definition
>5000	Very high velocity
4000–5000	High velocity
3500–4000	Middle velocity
2500–3500	Low velocity
<2500	Very low velocity

be interpreted by categorizations given in past work (Anon, 1979) (Table 3). The Particle size distribution was evaluated using a Malvern Mastersizer 2000 laser particle size analyser. This test was conducted on raw GP and slag, in addition to co-grinding GP and slag with solid chemicals (sodium hydroxide and sodium metasilicate). Scanning electron microscopy (SEM) analysis was also performed on raw materials, the dry powder produced after the grinding process, and geopolymer hardened geopolymer grouts using a ZEISS Gemini SEM 300. A Fourier transform infra-red (FTIR) study was performed between 450 and 2000 cm^{-1} to identify chemical bonds present in the hardened geopolymer grouts.

3. Results and discussions

3.1. Particles size analysis

The particle size is the primary factor controlling rheological and mechanical characteristics variance. The particle size distribution of GP and slag before and after mechanochemical activation is displayed in Figure 3. The d_{50} (mean size) of raw GP and slag was 209 μm and 22 μm , respectively, whereas the mean size of GP and slag was reduced to 66 μm and 15 μm , respectively, after 2 hours of grinding in a ball mill with sodium hydroxide and sodium metasilicate, as shown in Figure 3.

Scanning electron microscopy analysis (SEM) shows the microstructural characterisation of slag and GP precursors before and after mechanochemical activation (Figure 4). As shown in Figure 4a, the raw slag particles are non-uniform and heterogeneous, with sub-rounded to angular forms. The roughness and edges were observed in both the angular and bulk particles (Balamurugan et al., 2021). As shown in Figure 4b, most raw GP particles have irregular and angular shapes with smooth surface textures.

Figure 4c and 4d shows the microstructural analysis of slag and GP precursors obtained after 2 h of ball milling in the presence of chemical powder (NaOH and sodium metasilicate). After grinding, the slag and GP particles were coated with solid chemical powder (NaOH and Na_2SiO_3), which decreased the average size of the precursors and solid chemicals (Figure 4c and 4d). Nonetheless, the slag and GP particles still have angular and slightly deformed shape after the mechanochemical grinding. Furthermore, the surface area of the particles increased obviously during mechanochemical activation and resulted in a higher reaction rate of the geopolymeric precursors. Additionally, initial bonding between the particles was observed (Figure 4d) due to the addition of NaOH and sodium metasilicate, which may reflect the MG

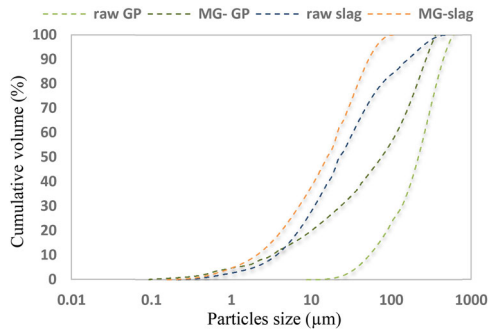


Figure 3. Particle size distribution of GP and slag before and after mechanochemical activation.

powder's adhesive nature. However, the effect of ball milling of all raw materials resulted in increased amorphousness and formation of the geopolymeric precursor (Gupta et al., 2017). Mukhtar et al. (2022a) reported that grinding of fly ash and slag with NaOH and sodium metasilicate for 2 h resulted in the formation of cracks and defects, which enhanced the surface roughness of the surface the particles and increased reactivity to the geopolymeric precursors.

3.2. Rheological behaviour and responses

The flow curves of geopolymer grouts activated by mechanochemical activation at varied NaOH concentrations are shown in Figure 5. Also, the dilatant index values (i.e. coefficient C) are presented in Table 4. All the MG grouts exhibited a shear thickening behaviour ($C > 0$). In other words, apparent viscosity increased as shear rate of grout increased, as illustrated in Figure 5. The experimental results demonstrate that the magnitudes of apparent viscosity and shear stress increased as the molarity of NaOH increased in all MG grouts. This behaviour is primarily attributed to the increase in the viscosity of the activation solution with NaOH concentration (Vance et al., 2014). Furthermore, low molarity negatively influenced the apparent viscosity due to the slow leaching rate of Al^{3+} and Si^{4+} (Vance et al., 2014; Palacios et al., 2019). Zhang et al., (2019) also reported that increasing the sodium hydroxide content (0.5 to 4 M) increased the viscosity of geopolymer-based grouts. This is due to the high reactivity of soluble aluminosilicate components, which accelerates polymerisation and hydration reactions, resulting in a rapid increase in viscosity of geopolymer mixture. On the other hand, the effect of GP content on the rheological responses of the fresh MG grout is presented in Figure 6. The flow curve showed that the MG grout containing 100% slag (MG-GP0) had the highest shear stress and apparent viscosity. In other words, a high slag amount increased the viscosity of the MG grout mixture due to the high reactivity of the slag binder, which results in the development of primary C-S-H gel during the initial stages of the reaction (Palacios et al., 2008). Additionally, the apparent viscosity and shear stress of the flow curves decreased dramatically as the GP content increased. This may be due to the comparatively smooth surface of GP particles, thereby reducing the water absorption, which is advantageous to reducing viscosity performance (Terro, 2006). According to Liang et al., (2021), workability (flowability) is associated with clusters in liquid suspensions. It has been shown that adding GP to geopolymer grout can reduce the formation of clusters (Jiang et al., 2020; Vafaei & Allahverdi, 2017), resulting in a decrease in the apparent viscosity of MG grout. Overall, the utilisation of glass powder is beneficial in terms of the rheological performance of geopolymer grouts.

In terms of geopolymer activation mechanism, the apparent viscosity and shear stress of CG grout were higher than MG grout, it can be concluded that CG grout mixtures mostly appear to produce higher magnitudes of apparent viscosity and shear stress in comparison to MG grout due to the high dissolution and ionisation degree of MG grout (Zhang et al., 2018). Similar behaviour was reported in the previous study by the authors of this article (Mukhtar et al., 2022a). Also, the magnitudes of shear stress and apparent viscosity of the MG grout were higher than those of the OPC grout, as illustrated in Figure 6. This could be due to the fact that the mechanochemical process alters the surface area and particle size of the powder; as a result, additional water is required to cover the surface of the particles, resulting

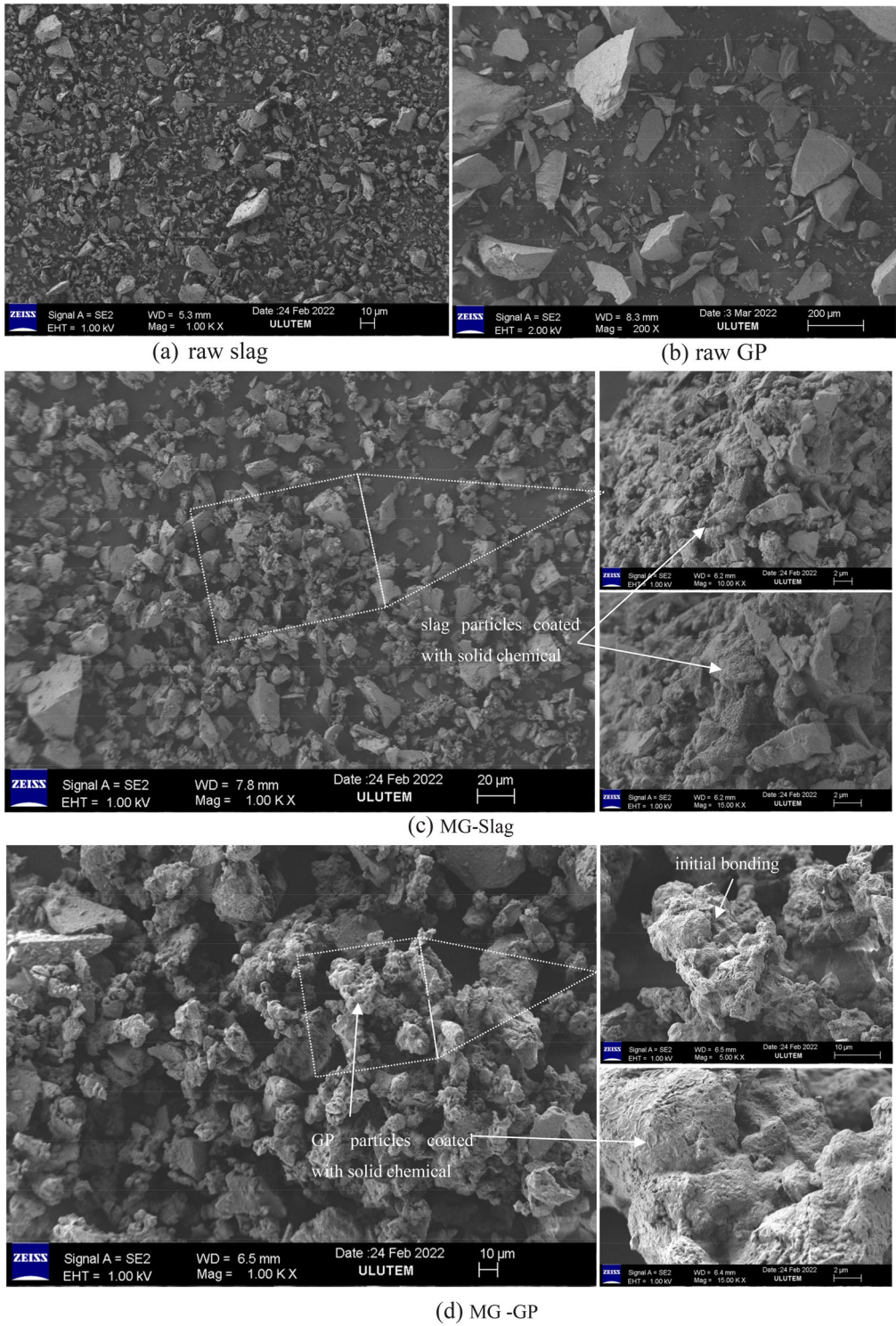


Figure 4. SEM micrographs of raw materials before and after mechanochemical process.

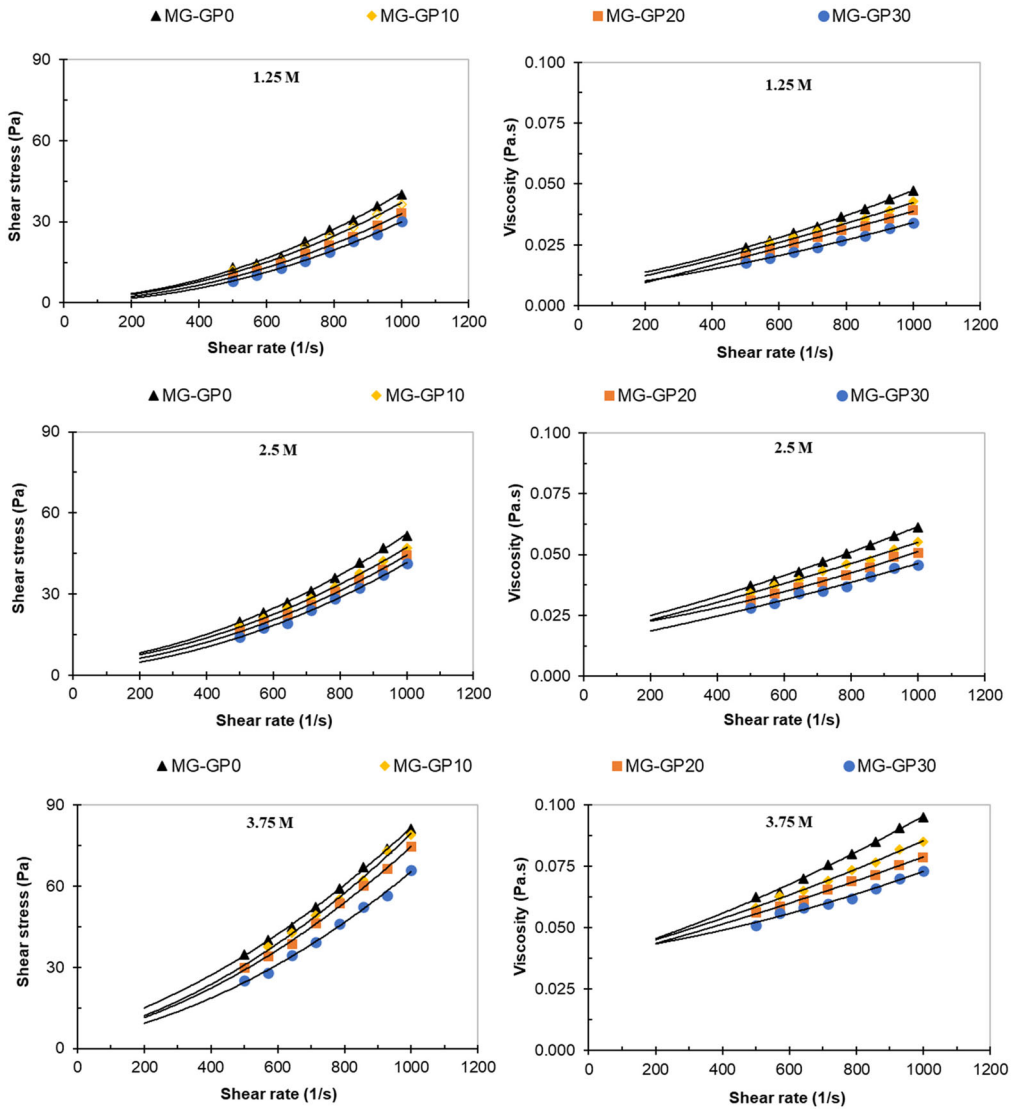


Figure 5. Flow responses curves of MG grout.

Table 4. Rheological characteristics of the grout.

Molarity	Mix ID	coefficient C	YS (Pa)	PV (Pa. s)
1.25	MG-GP0	0.00003	1.1	0.005
	MG-GP10	0.00003	0.95	0.0045
	MG-GP20	0.00003	0.48	0.0036
	MG-GP30	0.00003	0.35	0.0014
2.5	MG-GP0	0.00003	4.1	0.0138
	MG-GP10	0.00003	3.79	0.0127
	MG-GP20	0.00003	2.72	0.0116
	MG-GP30	0.00003	1.63	0.0099
3.75	MG-GP0	0.00004	5.8	0.038
	MG-GP10	0.00004	4.9	0.033
	MG-GP20	0.00004	3.85	0.03
	MG-GP30	0.00004	3.3	0.023
-	CG	0.00008	6.04	0.052
	OPC	0.00002	6.4	0.06

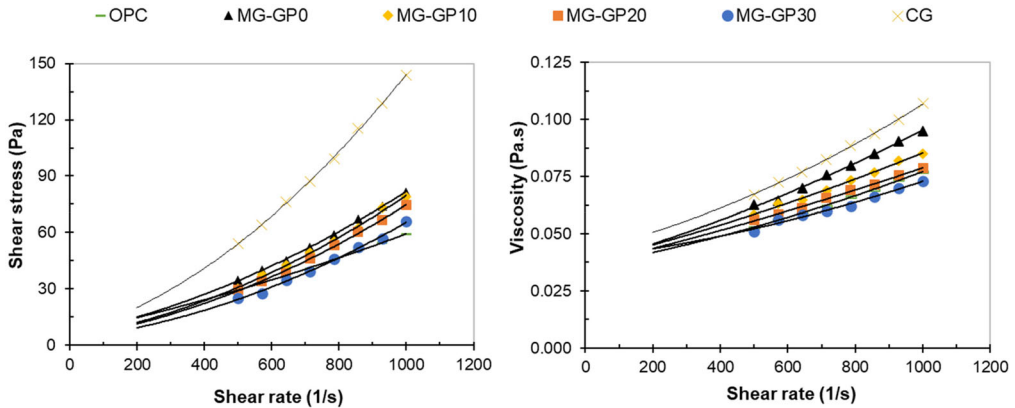


Figure 6. Flow responses curves of OPC, CG and MG grouts.

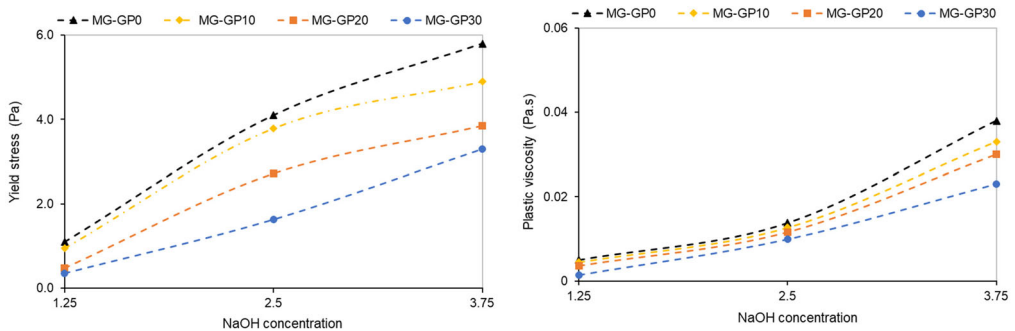


Figure 7. Effect of sodium hydroxide concentration on the yield stress and plastic viscosity of MG grouts.

in a remarkable reduction in free water in fresh grouts and an increase in the responses (shear stress and apparent viscosity) (Marjanović et al., 2014).

3.3. Yield stress and plastic viscosity

The yield stress (YS) and plastic viscosity (PV) of grouts were estimated using the modified Bingham model during rheological experiments. In general, both YS and PV increased with the increasing of NaOH concentration. As shown in Figure 7, the YS and PV values of MG grout were in the range of 1.1–0.35 Pa and 0.005–0.0014 Pa.s at 1.25 molarity and between 5.8–3.3 Pa and 0.038–0.023 Pa.s at 3.75 molarity, respectively, the increase in YS and PV has been mainly attributed to the use of a high concentration of sodium hydroxide resulting in higher storage modulus which indicates the presence of a rigid structure that leads to higher geopolymerisation kinetics (Lu et al., 2021). Similar findings were obtained by Rifaai et al. (2019) who indicated that the increase in NaOH concentration from 2 to 7 M increased the yield stress of alkali-activated slag pastes.

On the other hand, the YS and PV of the MG grout gradually decrease with increasing GP content (Table 4). The results showed that mixtures with 100% slag (MG -GP0) have higher YS and PV of 5.8 pa and 0.038 p.as, respectively (Figure 8). According to Palacios et al., (2008) the higher yield stress of high slag content mixtures may be explained by the mechanism governing the reaction; the slag particles are surrounded by a thin layer of primary C-S-H generated by the interaction of the silicate ions and the Ca^{2+} ions in the slag immediately after contact with the alkali activator. Under these conditions, colloidal forces attracted slag particles to one another, resulting in the formation of flocs. These flocs are partially separated during mixing and treatment before rheological testing; however, the rapid precipitation of massive amounts of primary C-S-H gel continues, generating larger flocs. As a result, the higher yield stress is required to initiate flow.

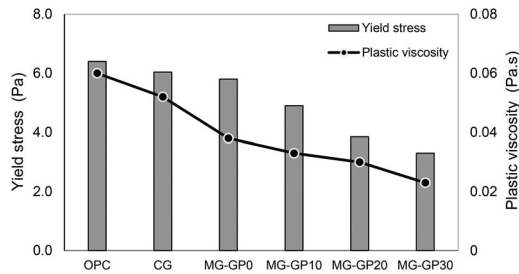


Figure 8. Yield stress and plastic viscosity of OPC, CG and MG grouts.

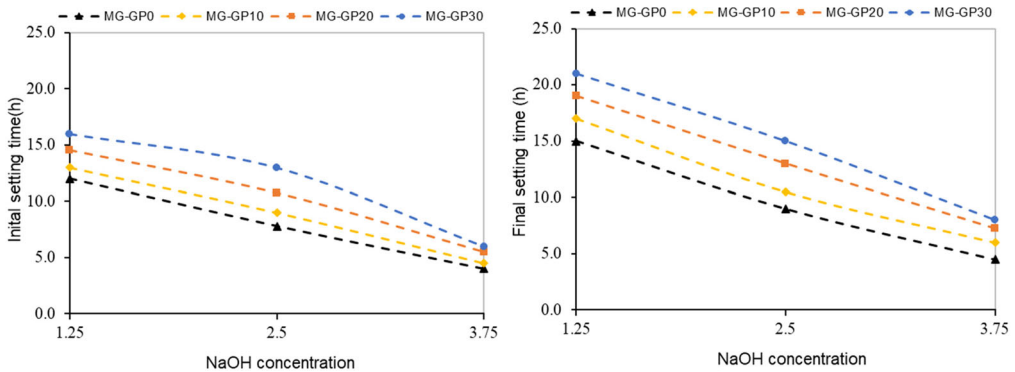


Figure 9. Influence of NaOH concentration on the setting time of MG-based grouts.

Also, incorporating GP in MG grout dramatically alters the reaction products and physicochemical interactions. The YS of MG-GP10, MG-GP20 and MG-GP30 grouts reduced by 16%, 34% and 43%, and the PV reduced by 13%, 21% and 39% when compared to MG-GP0, respectively. Glass powder has a lower surface area, a larger mean particle size, and a comparatively smooth surface. Thus, by including glass particles into the geopolymer grout, the demand for water to wet the solid precursors was decreased, leading to an increase in the amount of available water in the mixture during the fresh stage. The additional water in the glass powder-containing binder can act as a lubricant between the geopolymeric particles, thereby reducing the viscosity of fresh grouts (Si et al., 2020). Therefore, the YS and PV of the geopolymer grout decrease as the GP proportion of MG mixes increases.

The results also demonstrated that the YS and PV of the OPC grout were higher than those of the MG and CG grouts, as illustrated in Table 4. The YS and PV of MG-GP0 grout are 5.8 Pa and 0.038 Pa. s, respectively. In contrast, OPC grout has a YS and PV of 6.4 Pa and 0.06 Pa. s (Figure 8) because cement particles begin to hydrate and dissolve when they come into contact with water, creating positive and negative charges on the cement surface and inducing electrostatic attraction between the cement particles, leading to grouping or flocculation of the particles (Zhang et al., 2018). The hydration product ettringite was negatively charged in the synthetic pore solution (liquid phase of hydrating cement suspension), whereas calcium silicate hydrates and tricalcium silicate were positively charged (Zingg et al., 2008). Liang et al., (2021) reported that part of the water is wrapped in cement particles; therefore, a decrease in the amount of free water would be observed, increasing the effective solids volume fraction. However, in the MG grout, the silicate anions are absorbed on the surface of precursor particles like slag, generating negative charges on the particles' surfaces and resulting in electrostatic repulsion between them (Kashani et al., 2014). In other words, it had a reduced effective solid volume fraction, which resulted in lower YS and PV.

From the perspective of the activation method, the MG grout unveiled a lower YS and PV than the CG grout (Table 4). The YS and PV of MG grout are 4% and 27% less than the CG grout. This could be because the alkali activator solution dissolves rapidly at an early stage when blended with the raw materials that rich in alumina and silica to produce a conventional geopolymerisation reaction, which is significantly more viscous than the required water to form MG grout, resulting in a greater YS and PV of the CG grout

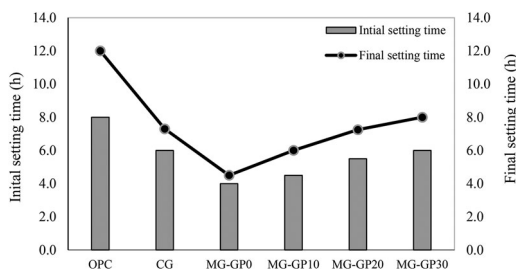


Figure 10. Setting time of OPC, CG and MG grouts.

(Mukhtar et al., 2022a). It is well known that a suspension's viscosity increases in direct proportion to the viscosity of the suspending solution (Konijn et al., 2014). It can be concluded that the higher YS and PV values are disadvantageous for grout when applied as a soil injection material, as the materials would be difficult to pump through the pipe if the slurry was overly viscous. Hence, MG grout is more suitable for soil injection applications than CG and OPC grout.

3.4. Fresh properties

3.4.1. Setting time

The setting time of MG grouts with varying sodium hydroxide concentrations is illustrated in Figure 9. The results revealed that the setting time was considerably shortened with the increasing molar concentration of NaOH, the initial setting time was shortened by 28% and 64%, respectively, at 2.5 and 3.75 molarity, as compared to 1.25 molarity. This is because the alkalinity of the sodium hydroxide solution causes the release of Al^{3+} , Ca^{2+} and Si^{4+} from slag and GP, which subsequently diffuse out of the geopolymerisation products that rapidly develop around unreacted particles during the leaching reaction. Alkaline conditions promote the activation reaction, whereas hydroxide accelerates slag and GP dissolution and also enhances aluminosilicate solubility (Marjanovi et al., 2014).

The effect of glass powder content on the setting times of MG grouts is depicted in Figure 10. In general, the addition of GP into geopolymer grouts considerably increased the setting time duration. The initial setting time of MG-GP10, MG-GP20 and MG-GP30 increased by 13%, 38% and 50%, respectively. Similarly, the final setting time increased by 33%, 61% and 78%, respectively, compared to MG-GP0. This is due mainly to the higher reaction rate of slag than GP, which leads to the formation of sodium, silicon and calcium components gels at an early stage of the reaction, accelerating the reaction process (Kumar et al., 2010). Furthermore, because the slag particles are much smaller than GP particles, the overall contact area between the solution and the solid particles decreases as the GP content in the system increases. As a result, the overall dissolving rate of the raw materials tended to be decreased during the reaction, resulting in a reduction in the polycondensation rate for samples that contain GP (Novais et al., 2016). Liang et al., (2021) reported that adding glass powder to metakaolin/fly ash-based geopolymer pastes significantly prolonged the setting time. On the other hand, the results demonstrated that the setting time of the MG grout was shorter than that of the OPC and CG grouts. The initial setting time of MG, CG and OPC was 4 h, 6 h and 8 h, and the final setting time was 4.5 h, 7.3 h and 12 h, respectively, under similar conditions, as seen in Figure 10. The shorter setting time of MG-GP0 grout could be attributed to mechanochemical mechanisms that create electronic charges on the surface of mechanochemically activated particles, resulting in a rise in surface energy and the transition from the crystalline to amorphous phase (Hosseini et al., 2021). Furthermore, the mechanochemical process disintegrates large alumina and silica particles, increasing their surface area and resulting in a more uniform distribution of particles in the mixture, which contributed to a higher proportion of additional alumina-silicate being formed from slag and GP, allowing for participation and dissolution in the formation of geopolymer gels (Mukhtar et al., 2022a; Marjanović et al., 2014). Thus, increased alumina-silicate availability accelerated the polymerisation process, resulting in creating an alumina-silicate gel network with extra alumina-silicate components. Due to the increased alumina-silicate crosslinking, the resulting gel has a more homogeneous microstructure, which results in a shorter setting time for MG-GP0 grout (Marjanović et al., 2014; Li et al., 2014). Li et al., (2020) noted that the setting time of the alkali activated slag/glass powder paste was much shorter than that of

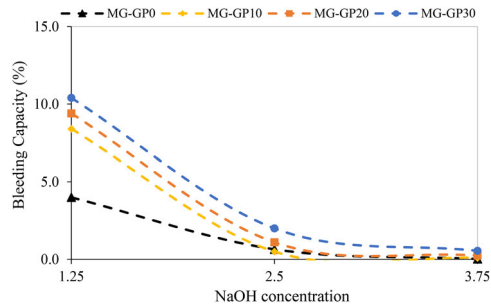


Figure 11. Effect of the sodium hydroxide concentration on the bleeding capacity of MG-based grout.

the OPC paste, and the time gap between the initial and the final setting was shorter. The longest setting time of the OPC mix is most likely due to the Portland cement being less reactive than the slag-based geopolymer grout, particularly in the early phases (Yi et al., 2015). The high reactivity of slag-based geopolymer tended to rapidly produce gels compared to OPC (Shang et al., 2018).

3.4.2. Bleeding capacity

Figure 11 shows the effect of the NaOH concentration on the bleeding capacity of the MG grout. The results revealed that the bleeding capacity of MG grouts declined steadily as the NaOH concentration increased from 1.25 M to 2.5 M; the lowest value of bleeding capacity of MG grouts was at 3.75 molar concentration due to the fact that as the molarity increased, the leached amount of alumina-silicate enhanced, and additional water was required to form geopolymer networks (Mukhtar et al., 2022a). Zhang et al., (2019) observed a similar trend for slag activated by sodium hydroxide solutions. A significant decrease in bleeding capacity was noted with an increase in the sodium hydroxide concentration in the grout mixture. This tendency clearly indicates that the sodium hydroxide concentration played a positive role in the bleeding capacity. In addition to molarity, the bleeding capacity of MG grout increased with the increase of GP level; hence, it can be clearly observed that the bleeding capacity of MG grout gradually increases with the increasing glass powder replacement, as illustrated in Figure 12. The results revealed that the mixes with 100% slag content had the lowest bleeding capability. For example, the bleeding capacity of MG grout increased from 0.025% to 0.55% when GP content increased from 0 to 30%. Because of the high demand for water in the geopolymerisation of slag particles (Liang et al., 2019; Zhu et al., 2021), dissolution heat flow increased as slag amount increased since slag possesses a faster dissolution rate than GP (Khan et al., 2021), leading to rapid growth synthesis of reaction products to create a rigid network. In comparison to slag, the high bleeding capacity of geopolymer grout incorporating GP can be attributed to its low water requirement and filling effect. In addition, the surface of GP particles is comparatively smooth, which reduces the amount of water absorbed (Terro, 2006). The results also showed that the MG grout (MG-GP0) had significantly less bleeding capacity than the OPC and CG grouts, as seen in Figure 12. Due to the increased surface area and reduced particle size of the mechanochemically activated powder, additional water is required to cover the particles' surfaces (Marjanović et al., 2014). In general, the results of this research indicated that the bleeding of MG and CG grouts is more stable than OPC grout. The higher bleeding capacity of the OPC mix is most likely related to the fact that the Portland cement is less reactive than the slag-based geopolymer grout, particularly during these early stages (Yi et al., 2015). On the other hand, apparent viscosity played a positive role in improving the stability of grouts (Yin et al., 2021). The higher apparent viscosity of slag-based geopolymer grout represents a better reaction between water and binder and a stronger agglutination; hence, for bleeding to occur, the water needs to overcome higher friction from the grout particles (Xie et al., 2013).

3.5. Mechanical properties

3.5.1. UCS

Figure 13 presents the effect of different molarities of MG grouts on UCS at 7 days and 28 days. The results indicated that the NaOH molarity significantly influenced the UCS values of MG specimens. In general, the UCS values of MG grout increased as the molarity of NaOH increased. For instance, the UCS of

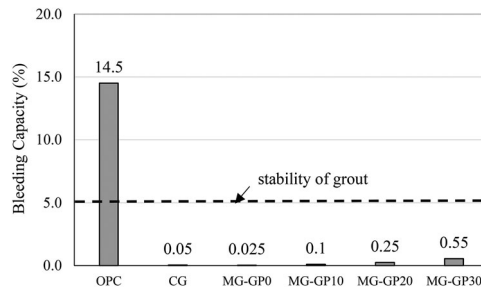


Figure 12. The bleeding capacity of OPC, CG and MG grouts.

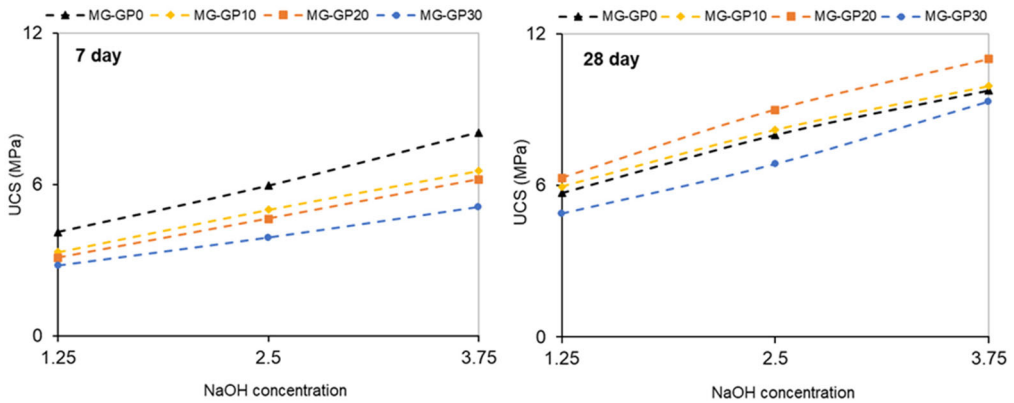


Figure 13. Effect of the sodium hydroxide concentration on the UCS of MG grouts.

MG-GP0 improved by 40% and 71%, respectively, whereas the UCS of MG-GP30 improved by 39% and 90% at 2.5 and 3.75 molarity, respectively, at 28 days. It can be concluded that the optimum UCS values were seen at 3.75 molarity among all the MG grouts. Strength enhancement is usually controlled by the amount of alumina silicate leached from the source materials; hence, increasing the molarity of NaOH results in increased Al^{3+} and Si^{4+} dissolved, resulting in a strong geopolymeric network (Zhang et al., 2019). Liang et al., (2021) also reported that the GP's active ions (Si^{4+} , Al^{3+} and Ca^{2+}) are dissolved and leached efficiently in the NaOH solution. Furthermore, dissolution of NaOH at low molarity indicated that OH^- ions were insufficient to break the Al-Si link, resulting in the formation of a few alumina silicate tetrahedral monomers. Whereas, at a high molar concentration of NaOH, OH ions completely broke all silicon-aluminum bonds and generated extra alumina silicate tetrahedral monomers, completing the dissolution. As a result, the microstructure of geopolymer grout was condensed, and the mechanical properties were increased (Abdullah et al., 2021; Muraleedharan & Nadir, 2021).

Figure 14 shows the effect of GP replacements on UCS values of MG specimens at 7 and 28 days. The UCS values of all studied mixtures improved as the age increased from 7 to 28 days; specimens cured at 28 days displayed better strength characteristics than specimens cured at 7 days due to the completion of the polymerisation process and densification of the microstructure at longer ages (Liang et al., 2019; Tho-In et al., 2018; Athira et al., 2021). On the other hand, the UCS results for MG grout samples containing GP revealed that the UCS increases with increased curing time, and fewer cracks on the surface of the specimens were observed compared to the MG-GP0 sample. The UCS test results of the MG grout reduced with increasing GP replacement level at 7 days after that, started to increase with increasing GP content up to 20% at 28 days, as shown in Figure 14. For instance, after 7 days of curing, the decreases in UCS were 18%, 23% and 37% for GP levels of 10%, 20% and 30%, respectively. Similar results were reported in previous research (Khan et al., 2021; Tho-In et al., 2018). The increase in UCS of MG-GP grout over time is due to the dissolving a notable proportion of silica from GP in an alkali media (Fernández-Jiménez et al., 2017), whereas the UCS of MG grout increased slightly at 10% GP, and the MG-GP20 mix exhibited the highest UCS at 20% GP replacement among all MG grouts after 28 days. The UCS of the MG-GP20 grout was 13% higher than that of the control mix (MG-GP0) because the major active ions

(Si^{4+} , Al^{3+} and Ca^{2+}) were dissolved and leached from GP in the alkaline activator, and the soluble ions contribute to the increased reactivity of solid precursors and participate further in the geopolymerisation reaction, hence increasing strengths (Liang et al., 2021; Jiang et al., 2020; Zhang et al., 2017). It is important to note that replacing slag with 30% GP decreased the UCS by 4% compared to MG-GP0. The higher amount of GP substantially impacted the silica-alumina ratio due to the high silicon concentration in GP. Silva et al., (2007) reported that the silica-alumina ratio had a substantial impact on the mechanical characteristics of the geopolymer. With a high silica-alumina ratio, low-crosslinked aluminosilicate materials with reduced strengths were developed (Tho-In et al., 2018). Furthermore, the relatively lower calcium oxide content in GP decreased the UCS because the high calcium oxide content in the geopolymer gel could create more hydrated products such as calcium silicate hydrate gel in addition to the three-dimensional matrix network (Lee & Lee, 2013), which lowered the UCS. Thus, it can be concluded that GP up to 20% can be used as a precursor for geopolymer synthesis after mechanochemical treatment.

From the perspective of the activation method, the mechanochemical mechanism had a considerable influence on the strength performance of MG grout specimens. The UCS values of CG grout were lower than its counterpart MG (Figure 14); the UCS was reduced by 18% compared to MG-GP0 due to the higher cracks observed at 28 days, as shown in Figure 15. Notably, the strength performance of the mixes containing 100% slag activated conventionally was reduced at longer curing period. The UCS of the CG grout sample was 8.7 MPa and 8 MPa at 7 days and 28 days, respectively. Moreover, the shape of the CG grout sample at 28 days revealed apparent micro-cracks on the surface of the specimen, as seen in Figure 15. These cracks can be attributed to the fact that there is more apparent shrinkage after 28 days compared to 7 days; this aspect contributes to the decrease in strength of CG samples after 28 days (Mukhtar et al., 2022a; Lee & Lee, 2013). Additionally, mechanochemical activation increased the surface area and reaction rate of slag; as a result, an extra gel was generated as a consequence of the main reaction, which then accumulated and filled the pore system. The formation of a large proportion of gel in the geopolymer mixture improved the overall pore volume and porosity of the geopolymer grout, resulting in enhanced immobilisation (Mukhtar et al., 2022a). Similar MG grout behaviour was reported in (Mukhtar et al., 2022b; Fernández-Jiménez et al., 2019; Adesanya et al., 2020). On the other hand, the results revealed that the USC of OPC sample was a little higher than that of the MG-GP0 and CG mixes

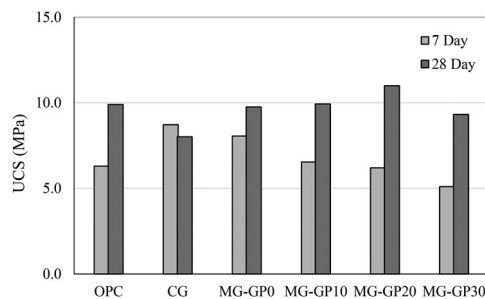


Figure 14. UCS of OPC, CG and MG grouts.

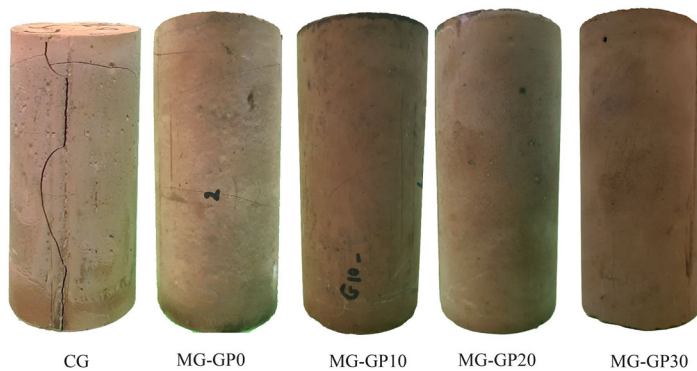


Figure 15. The visual appearance of CG and MG grouts at 3.75 M.

due to the high shrinkage of slag and lower calcium content compared to OPC. For example, the UCS of OPC is 1.4%, 19% higher than MG-GP0 and CG, and 10% lower than MG-GP20, respectively (Figure 14). It can be concluded that the UCS of MG-GP20 \geq OPC \geq CG grouts; therefore, the GP can be effectively used in mechanochemical geopolymer grout up to 20% replacement.

3.5.2. UPV

Figure 16 presents the influence of molarity on UPV tests for MG grouts at 7 and 28 days. It can be seen from Figure 16 that the UPV values of MG grout were enhanced significantly at the curing ages of 7 and 28 days. Based on the UPV classification presented in Table 3, all obtained specimens' hardened states ranged from low velocity to very low velocity (Anon, 1979). This indicates that the microstructure of hardened grout becomes denser as the curing period increases. It was observed that increasing NaOH concentration significantly influenced UPV measurements. In other words, the UPV increased as the molar concentration increased, and the highest UPV values were observed at 3.75 molarity. Moreover, the combined effect of sodium hydroxide concentration and glass powder content in geopolymer grout showed higher UPV values than those of control samples (MG-GP0). For instance, the UPV of MG-GP0, MG-GP10, MG-GP20 and MG-GP30 increased by 31%, 44%, 50% and 60% when the molarity of sodium hydroxide increased from 1.25 to 3.75 M, respectively due to the fact that the increasing NaOH concentration resulted in an increase in leaching conditions, including the quantity and rate of active ions (Al^{3+} and Si^{4+}), which constitute an important basis for GP as a precursor to participating in the geopolymerisation reaction. Thus, the leaching environment for these active ions in GP has an effect on the reaction kinetics, mechanical characteristics and microstructure formation of the geopolymer grout (Zhang et al., 2017). Besides, the UPV values of the MG grout increased noticeably at different GP contents (Figure 17). The UPV of the MG grout improved by 2% and 6% when the GP content increased from 10% to 20%. The improved performance of the UPV can be attributed to the integration of more silicon ions into the aluminosilicate network, which is provided by GP (Samarakoon et al., 2020). However, the UPV of MG-GP30 decreased by 1.5% when slag was replaced with 30% compared to the MG-GP20 mix. This reduction is due to an insufficient amount of calcium and alumina in the reaction systems, reducing the amount of precipitated C-(N-) A-S-H, which may explain why MG-GP30 had lower strengths than other mixtures (Samarakoon et al., 2020; Xiao et al., 2021). Additionally, the results reveal that the activation mechanism of geopolymer grout significantly affected the UPV values (Figure 17). The UPV values of MG samples were higher than CG samples because the grinding of the precursor led to a reduction in particle size and increased the surface area of the slag and GP particles, lowering the porosity and raising the density of the geopolymer grout. Additionally, the polymerisation process was significantly accelerated upon grinding due to the addition of aluminosilicate gel to the mixture, reducing the porosity and enhancing GP and slag particles (Kumar & Kumar, 2011).

3.6. Microstructural analysis

Figure 18 shows the effect of the activation method on the microstructure characterisation of MG and CG grouts. Notably, the activation method considerably impacts the microstructure of geopolymer grout. As seen in Figure 18a and 18b, many unreactive slag particles can be observed in CG grout as compared

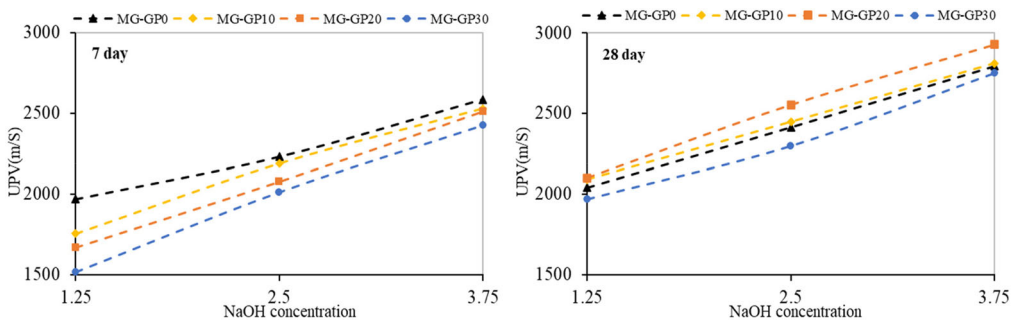


Figure 16. Effect of the NaOH concentration on the UPV of MG grout.

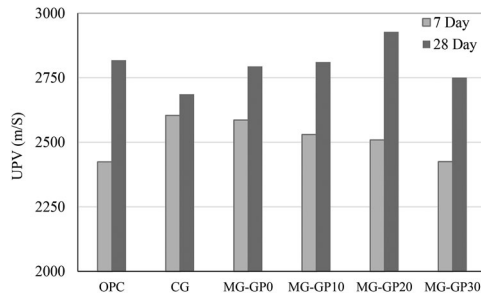
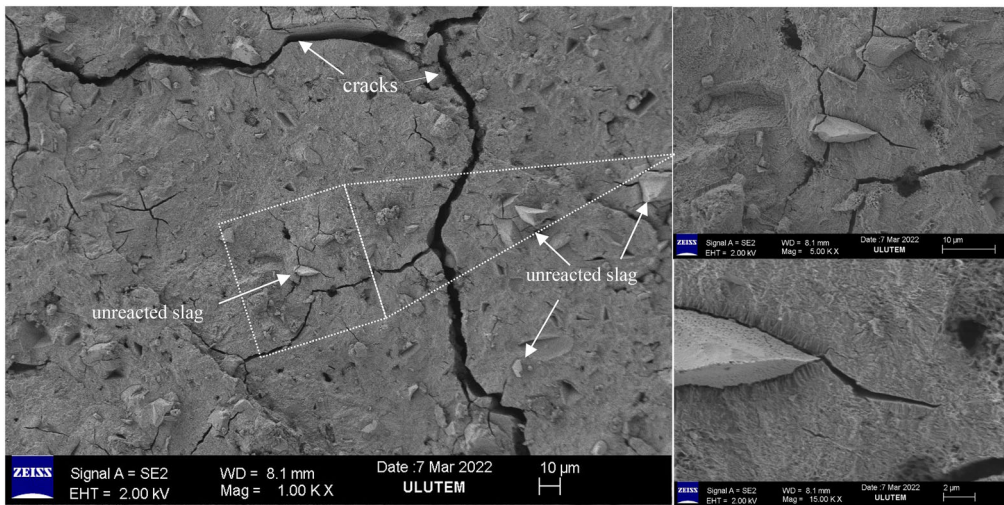
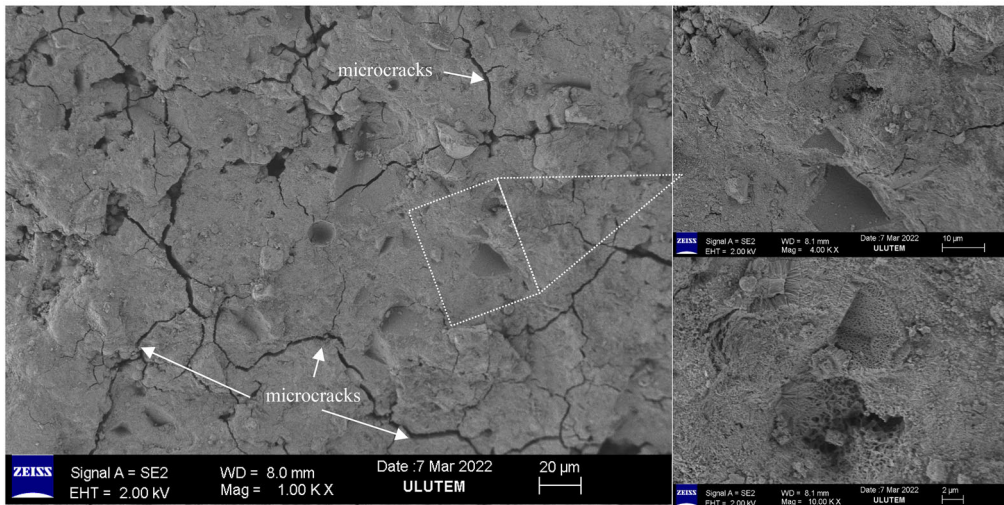


Figure 17. UPV of OPC, CG and MG grouts.



(a) CG

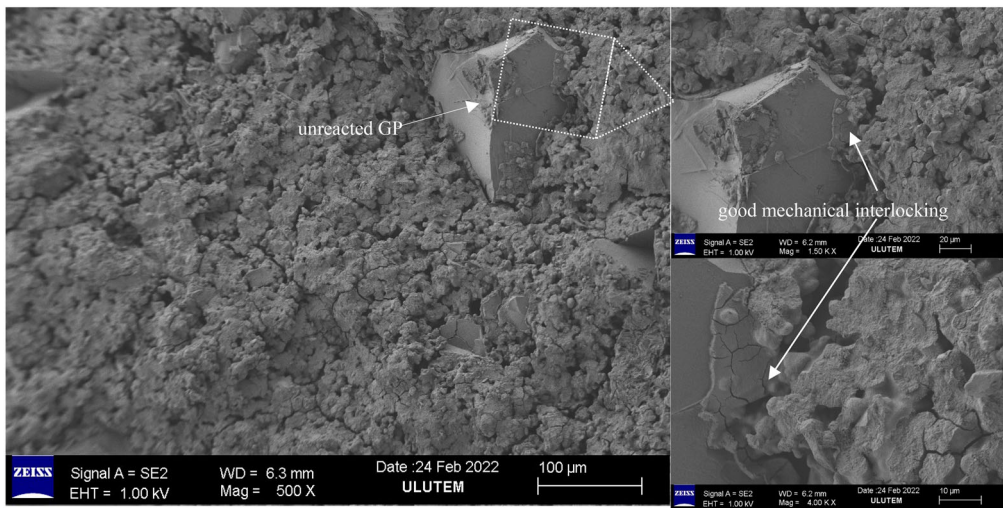


(b) MG-GP0

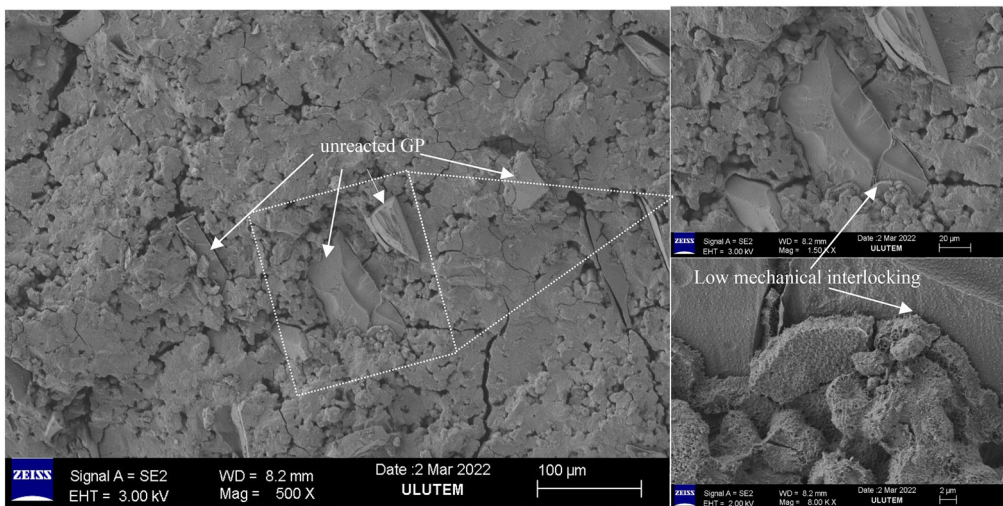
Figure 18. SEM images of the hardened (a) CG and (b) MG-GP0 grouts.

to its counterpart MG-GP0 which did not include any unreactive slag particles due to the beneficial effect of mechanochemical treatment that increased surface area and reduced the particle size of slag, resulting in lower porosity and higher density in comparison with slag based-CG grout. Additionally, significant

cracks can be seen in CG grout (Figure 18a) because of the poor connectivity of the reaction products (Mukhtar et al., 2022a). It can be indicated that the mechanochemical activation method is more beneficial than the conventional activation method in densifying the compactness of grout's microstructure, and thus, the mechanical properties of MG grout have been greatly enhanced. Furthermore, the geopolymerisation reaction of MG grout was dramatically enhanced during the ball milling process due to the creation of additional aluminosilicate gel in the mixture (Figure 18b); the produced gel has a more homogeneous microstructure which decreased the porosity and enhanced the reaction rate of slag particles (Abbas et al., 2023). Figure 19 presents the influence of glass powder contents on the microstructure characterisation of MG grout. The results indicated that the MG grout exhibited a more compact morphology with 20% GP replacements, and the reaction products became entirely completed. The number of non-reacted GP particles is limited, indicating that the inclusion of 20% GP promotes the formation of a highly dense microstructure (Figure 19a). In other words, the SEM micrographs of MG-GP20 displayed a high compactness microstructure with less pores and no visible cracks in comparison with MG-GP0 micrographs (Figure 18b) and MG-GP30 (Figure 19b). This reveals that 20% GP in MG grout led to the



(a) MG-GP20



(b) MG-GP30

Figure 19. SEM images of the hardened (a) MG-GP20 and (c) MG-GP30 grouts.

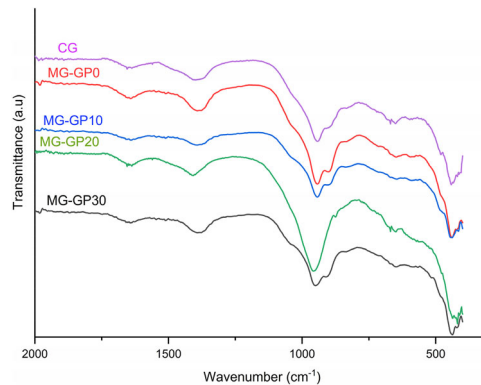


Figure 20. FTIR spectra of the hardened CG and MG grouts.

production of additional aluminosilicate gels due to more reactive SiO_2 participating in the geopolymerisation process (Khan et al., 2021; Samarakoon et al., 2020; Pascual et al., 2021). Similarly, Jiang et al., (2020) observed that the geopolymer paste specimens with 20% GP had better homogeneity due to reactive SiO_2 and Al_2O_3 , which contributed to the generation of hydrated sodium aluminosilicate gel (N–A–S–H). As a result, 20% slag replacement by glass powder improved the mechanical performance of slag-based MG grout. This observation shows a good agreement with previous studies (Khan et al., 2021; Liang et al., 2021). At 30% GP, the microstructure of the MG-GP30 is still denser and more compact than MG-GP0; however, it showed a significant number of unreacted GP particles with many microcracks (Figure 19b). These microcracks may occur as a result of an excess of GP, which reduces the production of crosslinking structures in reaction products. Due to the excessive amount of GP, the interface between the glass powder particles and the MG matrix was reduced. Therefore, the low mechanical interlocking and the formed microcracks resulted in lower densification and a lower mechanical performance of MG-GP30 samples compared to MG-GP20 samples, as shown in Figure 19b (Vásquez et al., 2016). This behaviour is related to the considerable decrease in alumina content as the GP content increases as alumina is required for the formation of a stable polymer network (Novais et al., 2016). Therefore, partial slag replacement with 30% GP decreased the UCS of the geopolymer grout used for mechanochemical activation.

The FTIR spectra for all the geopolymer grout at age of 28 days are presented in Figure 20. It apparently illustrates that a band associated with the vibrations of OH and H-OH at approximately 1640 and 2000 cm^{-1} , which was assigned to the existence of crystal or absorbed water produced during the reaction procedures. The strongest vibration of T-O-Si bonds at 900–1000 cm^{-1} (where T = tetrahedral Si or Al) could be attributed to the formation of gel phases (Zhang et al., 2017; Zhang et al., 2012; Zhu et al., 2019). This band indicates the presence of geopolymerisation resulting from the production of amorphous aluminosilicate phases; thus, this band can be used to determine the degree of polymerisation (Tho-In et al., 2018; Karim et al., 2013; Kumar et al., 2017). The FTIR spectrum reveals that the Si–O band at 940 cm^{-1} is more intense in the MG grout than in the CG grout, indicating that the mechanochemical activation method positively affected the geopolymerisation rate of geopolymer grout (Hosseini et al., 2021). On the other hand, the intensity of the Si–O stretching bands at 950 cm^{-1} becomes broader and more intense at a 20% GP replacement, owing to the formation of a more stable gel (Tho-In et al., 2018; Zhang et al., 2017). However, the wavenumber bands weaken in samples MG-GP30 with the more addition of GP, which indicates that the excessive GP content plays a negative role in the procedure of reaction and is unfavourable to the formation of gel phases. This result is consistent with the change in the unconfined compressive strength. That is to say, the addition of GP dosage should not be beyond 20%.

4. Conclusions

In this research, the effects of glass powder and molar concentration of NaOH on the performance of mechanochemical geopolymer grout were investigated. Also, a conventionally activated geopolymer-based grout and an ordinary Portland cement (OPC) grout were also investigated for comparison. The rheological, fresh,

mechanical and microstructural performances were examined for all obtained grouts. The conclusions were as follows:

- The apparent viscosity and shear stress of all MG grouts dramatically decreased with the increasing GP content, while increasing as the molarity of NaOH increased. The yield stress and plastic viscosity values of the MG grout were reduced by 16–43% and 13–39% when slag was substituted with 0–30% GP, respectively. Additionally, the yield stress and plastic viscosity of MG grouts increased as NaOH concentration increased. Furthermore, the mechanochemical activation method positively affected the rheological properties of geopolymer grouts.
- The use of 0–30% glass powder increased the initial and final setting time of MG grout between 33–50% and 33–78% as compared to the control mix (MG-GP0), respectively. On the contrary, the setting time was considerably shortened with mechanochemical activation and a higher molar concentration of NaOH.
- The bleeding capacity of MG grout increased from 0.025% to 0.55% when GP content increased from 0 to 30% due to its low water demand and filling impact compared to slag. Whereas the bleeding capacity of geopolymer grouts reduced as NaOH concentration increased. Moreover, the results also showed that the MG grout had significantly less bleeding capacity than the CG and OPC grouts.
- The substitution of 10–20% slag with glass powder enhanced the UCS of MG grouts by 2–13% due to introducing more active silicon into the geopolymerisation reaction process by glass powder, hence promoting the formation of additional gel phases. In addition, the UCS values of MG grouts increased in the range of 40–90% as the NaOH concentration increased from 1.25 to 3.75 M. Regarding the effect of the activation mechanism, the mechanochemical technique increased the strength of geopolymer grout by 18% in comparison to its conventional counterpart.
- The ultrasonic pulse velocity increased as GP content and sodium hydroxide molarity increased. The highest UPV was 2928 m/s for MG grout with 20% GP content and 3.75 M, at 28 days. Besides, the obtained results showed that the UPV of MG-GP20 \geq OPC \geq CG grouts; hence, it can be inferred that GP can be used efficiently in mechanochemically activated geopolymer grout up to 20% replacement.
- The microstructural analysis confirmed that the activation method had a measurable effect on the microstructure of geopolymer grout because of the grinding process increased the surface area and reduced the particle size of slag, resulting in lower porosity and higher density than conventionally activated geopolymer grout samples. Furthermore, the SEM images demonstrated that the microstructure of MG grout at 20% GP was densely compacted with less pores due to the enhanced polymerisation of reaction products inside the structure, which contributed to the formation of additional aluminosilicate gels.

Data availability statement (DAS)

The authors confirm that the data supporting the findings of this study are available within the article [and/or] its [supplementary materials](#).

Disclosure statement

No potential conflict of interest was reported by the authors.

References

- Abbas, I. S., Abed, M. H., & Canakci, H. (2023). Development and characterization of eco-and user-friendly grout production via mechanochemical activation of geopolymer. *Journal of Building Engineering*, 63, 105336. <https://doi.org/10.1016/j.jobbe.2022.105336>
- Abdullah, A., Hussin, K., Abdullah, M. M. A. B., Yahya, Z., Sochacki, W., Razak, R. A., Błoch, K., & Fansuri, H. (2021). The effects of various concentrations of NaOH on the inter-particle gelation of a fly ash geopolymer aggregate. *Materials (Basel)*, 14(5), 1111. <https://doi.org/10.3390/ma14051111>
- Adesanya, E., Ohenoja, K., Ylioniemi, J., & Illikainen, M. (2020). Mechanical transformation of phyllite mineralogy toward its use as alkali-activated binder precursor. *Minerals Engineering*, 145, 106093. <https://doi.org/10.1016/j.mineng.2019.106093>

- American Society for Testing & Materials. (1987). Standard test methods for felt, 1–8. <https://doi.org/10.1520/C0191-19.2>
- Anon, O. H. (1979). Classification of rocks and soils for engineering geological mapping. Part 1: rock and soil materials. *Bulletin of the International Association of Engineering Geology*, 19, 355–371.
- ASTM, C. (2009). *Standard test method for pulse velocity through concrete*. ASTM Int.
- ASTM:C940-10a. (2010). Standard Test Method for Expansion and Bleeding of Freshly Mixed Grouts for Preplaced-Aggregate Concrete in the Laboratory. *ASTM International*, i, 1–3. <https://doi.org/10.1520/C0940-16.2>
- ASTM:D2938–95. (1995). Standard test method for unconfined compressive strength of intact rock core specimens. ASTM International, West Conshohocken, PA, USA.
- Athira, V. S., Bahurudeen, A., Saljas, M., & Jayachandran, K. (2021). Influence of different curing methods on mechanical and durability properties of alkali activated binders. *Construction and Building Materials*, 299, 123963. <https://doi.org/10.1016/j.conbuildmat.2021.123963>
- Baalumurugan, J., Ganesh Kumar, V., Stalin Dhas, T., Taran, S., Nalini, S., Karthick, V., Ravi, M., & Govindaraju, K. (2021). Utilization of induction furnace steel slag based iron oxide nanocomposites for antibacterial studies. *SN Applied Sciences*, 3(3), 1–8. <https://doi.org/10.1007/s42452-021-04299-9>
- Baláz, P., Achimovičová, M., Baláz, M., Billik, P., Cherkezova-Zheleva, Z., Criado, J. M., Delogu, F., Dutková, E., Gaffet, E., Gotor, F. J., Kumar, R., Mitov, I., Rojac, T., Senna, M., Streletskii, A., & Wieczorek-Ciurawa, K. (2013). Hallmarks of mechanochemistry: from nanoparticles to technology. *Chemical Society Reviews*, 42(18), 7571–7637. <https://doi.org/10.1039/c3cs35468g>
- Bilondi, M. P., Toufigh, M. M., & Toufigh, V. (2018). Experimental investigation of using a recycled glass powder-based geopolymer to improve the mechanical behavior of clay soils. *Construction and Building Materials*, 170, 302–313. <https://doi.org/10.1016/j.conbuildmat.2018.03.049>
- Duxson, P., & Provis, J. L. (2008). Designing precursors for geopolymer cements. *Journal of the American Ceramic Society*, 91(12), 3864–3869. <https://doi.org/10.1111/j.1551-2916.2008.02787.x>
- Favier, A., Hot, J., Habert, G., Roussel, N., & d’Espinose de Lacaillerie, J.-B. (2014). Flow properties of MK-based geopolymer pastes. A comparative study with standard Portland cement pastes. *Soft Matter*, 10(8), 1134–1141. <https://doi.org/10.1039/c3sm51889b>
- Fernández-Jiménez, A., Cristelo, N., Miranda, T., & Palomo, Á. (2017). Sustainable alkali activated materials: Precursor and activator derived from industrial wastes. *The Journal of Cleaner Production*, 162, 1200–1209. <https://doi.org/10.1016/j.jclepro.2017.06.151>
- Fernández-Jiménez, A., Garcia-Lodeiro, I., Maltseva, O., & Palomo, A. (2019). Mechanical-chemical activation of coal fly ashes: An effective way for recycling and make cementitious materials. *Frontiers in Materials*, 6, 51. <https://doi.org/10.3389/fmats.2019.00051>
- Feys, D., Wallevik, J. E., Yahia, A., Khayat, K. H., & Wallevik, O. H. (2013). Extension of the Reiner–Riwlin equation to determine modified Bingham parameters measured in coaxial cylinders rheometers. *Materials and Structures*, 46(1–2), 289–311. <https://doi.org/10.1617/s11527-012-9902-6>
- Fluids, C. (2003). Standard test method for viscosity of chemical grouts by brookfield viscometer. *Annual Book of ASTM Standards*, 04, 8–10. <https://doi.org/10.1520/D4016-08.2>
- Güllü, H. (2016). Comparison of rheological models for jet grout cement mixtures with various stabilizers. *Construction and Building Materials*, 127, 220–236. <https://doi.org/10.1016/j.conbuildmat.2016.09.129>
- Güllü, H., & Agha, A. A. (2021). The rheological, fresh and strength effects of cold-bonded geopolymer made with metakaolin and slag for grouting. *Construction and Building Materials*, 274, 122091. <https://doi.org/10.1016/j.conbuildmat.2020.122091>
- Güllü, H., Al Nuaimi, M. M. D., & Aytek, A. (2021). Rheological and strength performances of cold-bonded geopolymer made from limestone dust and bottom ash for grouting and deep mixing. *Bulletin of Engineering Geology and the Environment*, 80(2), 1103–1123. <https://doi.org/10.1007/s10064-020-01998-2>
- Gupta, R., Bhardwaj, P., Mishra, D., Mudgal, M., Chouhan, R. K., Prasad, M., & Amritphale, S. S. (2017). Evolution of advanced geopolymeric cementitious material via a novel process. *Advances in Cement Research*, 29(3), 125–134. <https://doi.org/10.1680/jadcr.16.00113>
- Güllü, H., Cevik, A., Al-Ezzi, K., M. A., & Gülsan, M. E. (2019). On the rheology of using geopolymer for grouting: A comparative study with cement-based grout included fly ash and cold bonded fly ash. *Construction and Building Materials*, 196, 594–610. <https://doi.org/10.1016/j.conbuildmat.2018.11.140>

- Mukhtar, H. A., Abbas, I. S., & Canakci, H. (2022a). Influence of mechanochemical activation on the rheological, fresh, and mechanical properties of one-part geopolymer grout. *Advances in Cement Research*, 1–15. <https://doi.org/10.1680/jadcr.21.00205>
- Mukhtar, H. A., Sabbar Abbas, I., Hamed, M., & Canakci, H. (2022b). Rheological, fresh, and mechanical properties of mechanochemically activated geopolymer grout: A comparative study with conventionally activated geopolymer grout. *Construction and Building Materials*, 322, 126338. <https://doi.org/10.1016/j.conbuildmat.2022.126338>
- Hosseini, S., Brake, N. A., Nikookar, M., Günaydın-Şen, Ö., & Snyder, H. A. (2021). Mechanochemically activated bottom ash-fly ash geopolymer. *Cement and Concrete Composites*, 118, 103976. <https://doi.org/10.1016/j.cemconcomp.2021.103976>
- Humur, G., & Çevik, A. (2022). Effects of hybrid fibers and nanosilica on mechanical and durability properties of lightweight engineered geopolymer composites subjected to cyclic loading and heating–cooling cycles. *Construction and Building Materials*, 326, 126846. <https://doi.org/10.1016/j.conbuildmat.2022.126846>
- Humur, G., & Çevik, A. (2022). Mechanical characterization of lightweight engineered geopolymer composites exposed to elevated temperatures. *Ceramics International*, 48(10), 13634–13650. <https://doi.org/10.1016/j.ceramint.2022.01.243>
- Intini, G., Liberti, L., Notarnicola, M., & Canio, F. D. (2009). Mechanochemical activation of coal fly ash for production of high strength cement conglomerates. *Химия в Интерессах Устойчивого Развития*, 17, 567–571.
- Jiang, X., Xiao, R., Ma, Y., Zhang, M., Bai, Y., & Huang, B. (2020). Influence of waste glass powder on the physico-mechanical properties and microstructures of fly ash-based geopolymer paste after exposure to high temperatures. *Construction and Building Materials*, 262, 120579. <https://doi.org/10.1016/j.conbuildmat.2020.120579>
- Juenger, M. C. G., Winnefeld, F., Provis, J. L., & Ideker, J. H. (2011). Advances in alternative cementitious binders. *Cement and Concrete Research*, 41(12), 1232–1243. <https://doi.org/10.1016/j.cemconres.2010.11.012>
- Karim, M. R., Zain, M. F. M., Jamil, M., & Lai, F. C. (2013). Fabrication of a non-cement binder using slag, palm oil fuel ash and rice husk ash with sodium hydroxide. *Construction and Building Materials*, 49, 894–902. <https://doi.org/10.1016/j.conbuildmat.2013.08.077>
- Kashani, A., Provis, J. L., Qiao, G. G., & Van Deventer, J. S. J. (2014). The interrelationship between surface chemistry and rheology in alkali activated slag paste. *Construction and Building Materials*, 65, 583–591. <https://doi.org/10.1016/j.conbuildmat.2014.04.127>
- Khan, M. N. N., Kuri, J. C., & Sarker, P. K. (2021). Effect of waste glass powder as a partial precursor in ambient cured alkali activated fly ash and fly ash-GGBFS mortars. *Journal of Building Engineering*, 34, 101934. <https://doi.org/10.1016/j.jobbe.2020.101934>
- Konijn, B. J., Sanderink, O. B. J., & Kruyt, N. P. (2014). Experimental study of the viscosity of suspensions: Effect of solid fraction, particle size and suspending liquid. *Powder Technology*, 266, 61–69. <https://doi.org/10.1016/j.powtec.2014.05.044>
- Kumar, S., & Kumar, R. (2011). Mechanical activation of fly ash: Effect on reaction, structure and properties of resulting geopolymer. *Ceramics International*, 37(2), 533–541. <https://doi.org/10.1016/j.ceramint.2010.09.038>
- Kumar, S., Kumar, R., & Mehrotra, S. P. (2010). Influence of granulated blast furnace slag on the reaction, structure and properties of fly ash based geopolymer. *Journal of Materials Science*, 45(3), 607–615. <https://doi.org/10.1007/s10853-009-3934-5>
- Kumar, S., Mucsi, G., Kristály, F., & Pekker, P. (2017). Mechanical activation of fly ash and its influence on micro and nano-structural behaviour of resulting geopolymers. *Advanced Powder Technology*, 28(3), 805–813. <https://doi.org/10.1016/j.apt.2016.11.027>
- Kushwah, S., Mudgal, M., & Chouhan, R. K. (2021). The process, characterization and mechanical properties of fly ash-based Solid form geopolymer via mechanical activation. *South African Journal of Chemical Engineering*, 38, 104–114. <https://doi.org/10.1016/j.sajce.2021.09.002>
- Lee, N. K., & Lee, H. K. (2013). Setting and mechanical properties of alkali-activated fly ash/slag concrete manufactured at room temperature. *Construction and Building Materials*, 47, 1201–1209. <https://doi.org/10.1016/j.conbuildmat.2013.05.107>

- Lee, W. K. W., & Van Deventer, J. S. J. (2002). Structural reorganisation of class F fly ash in alkaline silicate solutions. *Colloids and Surfaces A: Physicochemical and Engineering Aspects*, 211(1), 49–66. [https://doi.org/10.1016/S0927-7757\(02\)00237-6](https://doi.org/10.1016/S0927-7757(02)00237-6)
- Lee, W. K. W., & Van Deventer, J. S. J. (2003). Use of infrared spectroscopy to study geopolymerization of heterogeneous amorphous aluminosilicates. *Langmuir*, 19(21), 8726–8734. <https://doi.org/10.1021/la026127e>
- Li, H., Xu, D., Feng, S., & Shang, B. (2014). Microstructure and performance of fly ash micro-beads in cementitious material system. *Construction and Building Materials*, 52, 422–427. <https://doi.org/10.1016/j.conbuildmat.2013.11.040>
- Li, L., Lu, J. X., Zhang, B., & Poon, C. S. (2020). Rheology behavior of one-part alkali activated slag/glass powder (AASG) pastes. *Construction and Building Materials*, 258, 120381. <https://doi.org/10.1016/j.conbuildmat.2020.120381>
- Liang, G., Li, H., Zhu, H., Liu, T., Chen, Q., & Guo, H. (2021). Reuse of waste glass powder in alkali-activated metakaolin/fly ash pastes: Physical properties, reaction kinetics and microstructure. *Resources, Conservation and Recycling*, 173, 105721. <https://doi.org/10.1016/j.resconrec.2021.105721>
- Liang, G., Zhu, H., Zhang, Z., Wu, Q., & Du, J. (2019). Investigation of the waterproof property of alkali-activated metakaolin geopolymer added with rice husk ash. *The Journal of Cleaner Production*, 230, 603–612. <https://doi.org/10.1016/j.jclepro.2019.05.111>
- Liu, Y., Shi, C., Zhang, Z., & Li, N. (2019). An overview on the reuse of waste glasses in alkali-activated materials. *Resources, Conservation and Recycling*, 144, 297–309. <https://doi.org/10.1016/j.resconrec.2019.02.007>
- Lu, C., Zhang, Z., Shi, C., Li, N., Jiao, D., & Yuan, Q. (2021). Rheology of alkali-activated materials: A review. *Cement and Concrete Composites*, 121, 104061. <https://doi.org/10.1016/j.cemconcomp.2021.104061>
- Marjanovi, N., Komljenovi, M., Ba, Z., Nikoli, V., & Petrovi, R. (2014). Physical—mechanical and microstructural properties of alkali-activated fly ash—Blast furnace slag blends. <https://doi.org/10.1016/j.ceramint.2014.09.075>
- Marjanović, N., Komljenović, M., Baščarević, Z., & Nikolić, V. (2014). Improving reactivity of fly ash and properties of ensuing geopolymers through mechanical activation. *Construction and Building Materials*, 57, 151–162. <https://doi.org/10.1016/j.conbuildmat.2014.01.095>
- Masi, G., Filipponi, A., & Bignozzi, M. C. (2021). Fly ash-based one-part alkali activated mortars cured at room temperature: effect of precursor pre-treatments. *Open Ceram*, 8, 100178. <https://doi.org/10.1016/j.oceram.2021.100178>
- Matakah, F., Xu, L., Wu, W., & Soroushian, P. (2017). Mechanochemical synthesis of one-part alkali aluminosilicate hydraulic cement. *Materials and Structures*, 50(1), 1–12. <https://doi.org/10.1617/s11527-016-0968-4>
- Muraleedharan, M., & Nadir, Y. (2021). Factors affecting the mechanical properties and microstructure of geopolymers from red mud and granite waste powder: A review. *Ceramics International*, 47(10), 13257–13279. <https://doi.org/10.1016/j.ceramint.2021.02.009>
- Nedunuri, A., & Muhammad, S. (2020). Influential parameters in rheology of alkali-activated binders. *ACI Materials Journal*, 117, 75–85. <https://doi.org/10.14359/51724593>
- Novais, R. M., Ascensão, G., Seabra, M. P., & Labrincha, J. A. (2016). Waste glass from end-of-life fluorescent lamps as raw material in geopolymers. *Waste Management (New York, N.Y.)*, 52, 245–255. <https://doi.org/10.1016/j.wasman.2016.04.003>
- Pacheco-Torgal, F., Moura, D., Ding, Y., & Jalali, S. (2011). Composition, strength and workability of alkali-activated metakaolin based mortars. *Construction and Building Materials*, 25(9), 3732–3745. <https://doi.org/10.1016/j.conbuildmat.2011.04.017>
- Palacios, M., Alonso, M. M., Varga, C., & Puertas, F. (2019). Influence of the alkaline solution and temperature on the rheology and reactivity of alkali-activated fly ash pastes. *Cement and Concrete Composites*, 95, 277–284. <https://doi.org/10.1016/j.cemconcomp.2018.08.010>
- Palacios, M., Banfill, P. F. G., & Puertas, F. (2008). Rheology and setting of alkali-activated slag pastes and mortars: Effect of organic admixture. *ACI Materials Journal*, 105, 140.
- Park, C. K., Noh, M. H., & Park, T. H. (2005). Rheological properties of cementitious materials containing mineral admixtures. *Cement and Concrete Research*, 35(5), 842–849. <https://doi.org/10.1016/j.cemconres.2004.11.002>

- Pascual, A. B., Tognonvi, T. M., & Tagnit-Hamou, A. (2021). Optimization study of waste glass powder-based alkali activated materials incorporating metakaolin: Activation and curing conditions. *The Journal of Cleaner Production*, 308, 127435. <https://doi.org/10.1016/j.jclepro.2021.127435>
- Provis, J. L. (2009). Activating solution chemistry for geopolymers. *Geopolymers*, 50–71. <https://doi.org/10.1533/9781845696382.1.50>
- Rifaai, Y., Yahia, A., Mostafa, A., Aggoun, S., & Kadri, E. H. (2019). Rheology of fly ash-based geopolymer: Effect of NaOH concentration. *Construction and Building Materials*, 223, 583–594. <https://doi.org/10.1016/j.conbuildmat.2019.07.028>
- Şahmaran, M. (2008). The effect of replacement rate and fineness of natural zeolite on the rheological properties of cement-based grouts. *Canadian Journal of Civil Engineering*, 35(8), 796–806. <https://doi.org/10.1139/L08-039>
- Samarakoon, M. H., Ranjith, P. G., & De Silva, V. R. S. (2020). Effect of soda-lime glass powder on alkali-activated binders: Rheology, strength and microstructure characterization. *Construction and Building Materials*, 241, 118013. <https://doi.org/10.1016/j.conbuildmat.2020.118013>
- Shang, J., Dai, J., Zhao, T., Guo, S., Zhang, P., & Mu, B. (2018). Alternation of traditional cement mortars using fly ash-based geopolymer mortars modified by slag. *The Journal of Cleaner Production*, 203, 746–756. <https://doi.org/10.1016/j.jclepro.2018.08.255>
- Si, R., Guo, S., Dai, Q., & Wang, J. (2020). Atomic-structure, microstructure and mechanical properties of glass powder modified metakaolin-based geopolymer. *Construction and Building Materials*, 254, 119303. <https://doi.org/10.1016/j.conbuildmat.2020.119303>
- Silva, P. D., Sagoe-Crenstil, K., & Sirivivatnanon, V. (2007). Kinetics of geopolymerization: Role of Al₂O₃ and SiO₂. *Cement and Concrete Research*, 37(4), 512–518. <https://doi.org/10.1016/j.cemconres.2007.01.003>
- Souri, A., Kazemi-Kamyab, H., Snellings, R., Naghizadeh, R., Golestani-Fard, F., & Scrivener, K. (2015). Pozzolanic activity of mechanochemically and thermally activated kaolins in cement. *Cement and Concrete Research*, 77, 47–59. <https://doi.org/10.1016/j.cemconres.2015.04.017>
- Temuujin, J., Williams, R. P., & Van Riessen, A. (2009). Effect of mechanical activation of fly ash on the properties of geopolymer cured at ambient temperature. *Journal of Materials Processing Technology*, 209(12–13), 5276–5280. <https://doi.org/10.1016/j.jmatprotec.2009.03.016>
- Terro, M. J. (2006). Properties of concrete made with recycled crushed glass at elevated temperatures. *Building and Environment*, 41(5), 633–639. <https://doi.org/10.1016/j.buildenv.2005.02.018>
- Tho-In, T., Sata, V., Boonserm, K., & Chindaprasit, P. (2018). Compressive strength and microstructure analysis of geopolymer paste using waste glass powder and fly ash. *The Journal of Cleaner Production*, 172, 2892–2898. <https://doi.org/10.1016/j.jclepro.2017.11.125>
- Vafaei, M., & Allahverdi, A. (2017). High strength geopolymer binder based on waste-glass powder. *Advanced Powder Technology*, 28(1), 215–222. <https://doi.org/10.1016/j.apt.2016.09.034>
- Vance, K., Dakhane, A., Sant, G., & Neithalath, N. (2014). Observations on the rheological response of alkali activated fly ash suspensions: The role of activator type and concentration. *Rheologica Acta*, 53(10–11), 843–855. <https://doi.org/10.1007/s00397-014-0793-z>
- Vásquez, A., Cárdenas, V., Robayo, R. A., & de Gutiérrez, R. M. (2016). Geopolymer based on concrete demolition waste. *Advanced Powder Technology*, 27(4), 1173–1179. <https://doi.org/10.1016/j.apt.2016.03.029>
- Widjaja, B., & Lee, S. H.-H. (2013). Flow box test for viscosity of soil in plastic and viscous liquid states. *Soils Found*, 53(1), 35–46. <https://doi.org/10.1016/j.sandf.2012.12.002>
- Xiao, R., Ma, Y., Jiang, X., Zhang, M., Zhang, Y., Wang, Y., Huang, B., & He, Q. (2020). Strength, microstructure, efflorescence behavior and environmental impacts of waste glass geopolymers cured at ambient temperature. *The Journal of Cleaner Production*, 252, 119610. <https://doi.org/10.1016/j.jclepro.2019.119610>
- Xiao, R., Polaczyk, P., Zhang, M., Jiang, X., Zhang, Y., Huang, B., & Hu, W. (2020). Evaluation of glass powder-based geopolymer stabilized road bases containing recycled waste glass aggregate. *Transportation Research Record: Journal of the Transportation Research Board*, 2674(1), 22–32. <https://doi.org/10.1177/0361198119898695>
- Xiao, R., Zhang, Y., Jiang, X., Polaczyk, P., Ma, Y., & Huang, B. (2021). Alkali-activated slag supplemented with waste glass powder: Laboratory characterization, thermodynamic modelling and sustainability analysis. *The Journal of Cleaner Production*, 286, 125554. <https://doi.org/10.1016/j.jclepro.2020.125554>

- Xie, H., Liu, F., Fan, Y., Yang, H., Chen, J., Zhang, J., & Zuo, C. (2013). Workability and proportion design of pumping concrete based on rheological parameters. *Construction and Building Materials*, 44, 267–275. <https://doi.org/10.1016/j.conbuildmat.2013.02.051>
- Yahia, A., & Khayat, K. H. (2001). Analytical models for estimating yield stress of high-performance pseudoplastic grout. *Cement and Concrete Research*, 31(5), 731–738. [https://doi.org/10.1016/S0008-8846\(01\)00476-8](https://doi.org/10.1016/S0008-8846(01)00476-8)
- Yahia, A., Mantellato, S., & Flatt, R. J. (2016). Concrete rheology: A basis for understanding chemical admixtures. *Science and Technology of Concrete Admixtures* (pp. 97–127). Elsevier.
- Yi, Y., Zheng, X., Liu, S., & Al-Tabbaa, A. (2015). Comparison of reactive magnesia-and carbide slag-activated ground granulated blastfurnace slag and Portland cement for stabilisation of a natural soil. *Applied Clay Science*, 111, 21–26. <https://doi.org/10.1016/j.clay.2015.03.023>
- Yin, W., Li, X., Sun, T., Chen, Y., Xu, F., Yan, G., Xu, M., & Tian, K. (2021). Utilization of waste glass powder as partial replacement of cement for the cementitious grouts with superplasticizer and viscosity modifying agent binary mixtures: Rheological and mechanical performances. *Construction and Building Materials*, 286, 122953. <https://doi.org/10.1016/j.conbuildmat.2021.122953>
- Zhang, D. W., Min Wang, D., Liu, Z., & Zhu Xie, F. (2018). Rheology, agglomerate structure, and particle shape of fresh geopolymer pastes with different NaOH activators content. *Construction and Building Materials*, 187, 674–680. <https://doi.org/10.1016/j.conbuildmat.2018.07.205>
- Zhang, J., Li, S., Li, Z., Zhang, Q., Li, H., Du, J., & Qi, Y. (2019). Properties of fresh and hardened geopolymer-based grouts. *Ceramics—Silikaty*, 63, 164–173. <https://doi.org/10.13168/cs.2019.0008>
- Zhang, S., Keulen, A., Arbi, K., & Ye, G. (2017). Waste glass as partial mineral precursor in alkali-activated slag/fly ash system. *Cement and Concrete Research*, 102, 29–40. <https://doi.org/10.1016/j.cemconres.2017.08.012>
- Zhang, Y., Luo, X., Kong, X., Wang, F., & Gao, L. (2018). Rheological properties and microstructure of fresh cement pastes with varied dispersion media and superplasticizers. *Powder Technology*, 330, 219–227. <https://doi.org/10.1016/j.powtec.2018.02.014>
- Zhang, Y., Xiao, R., Jiang, X., Li, W., Zhu, X., & Huang, B. (2020). Effect of particle size and curing temperature on mechanical and microstructural properties of waste glass-slag-based and waste glass-fly ash-based geopolymers. *The Journal of Cleaner Production*, 273, 122970. <https://doi.org/10.1016/j.jclepro.2020.122970>
- Zhang, Z., Wang, H., & Provis, J. L. (2012). Quantitative study of the reactivity of fly ash in geopolymerization by FTIR. *Journal of Sustainable Cement-Based Materials*, 1(4), 154–166. <https://doi.org/10.1080/21650373.2012.752620>
- Zhu, H., Liang, G., Li, H., Wu, Q., Zhang, C., Yin, Z., & Hua, S. (2021). Insights to the sulfate resistance and microstructures of alkali-activated metakaolin/slag pastes. *Applied Clay Science*, 202, 105968. <https://doi.org/10.1016/j.clay.2020.105968>
- Zhu, H., Liang, G., Xu, J., Wu, Q., & Zhai, M. (2019). Influence of rice husk ash on the waterproof properties of ultrafine fly ash based geopolymer. *Construction and Building Materials*, 208, 394–401. <https://doi.org/10.1016/j.conbuildmat.2019.03.035>
- Zingg, A., Winnefeld, F., Holzer, L., Pakusch, J., Becker, S., & Gauckler, L. (2008). Adsorption of polyelectrolytes and its influence on the rheology, zeta potential, and microstructure of various cement and hydrate phases. *Journal of Colloid and Interface Science*, 323(2), 301–312. <https://doi.org/10.1016/j.jcis.2008.04.052>